

(*p*-cymene)Ruthenium(II)(diphenylphosphino)alkyne Complexes: Preparation of (μ -Cl)(μ -PPh₂C≡CR)-Bridged Ru/Pt Heterobimetallic Complexes

Jesús R. Berenguer,[†] María Bernechea,[†] Juan Forniés,^{*,‡} Ana García,[†] and Elena Lalinde^{*,†}

Departamento de Química, Grupo de Síntesis Química de La Rioja, UA-CSIC, Universidad de La Rioja, 26006, Logroño, Spain, and Departamento de Química Inorgánica, Instituto de Ciencia de Materiales de Aragón, Universidad de Zaragoza-Consejo Superior de Investigaciones Científicas, 50009 Zaragoza, Spain

Received May 6, 2004

The neutral complexes [η^6 -*p*-cymene)RuCl₂(PPh₂C≡CR)] (R = Ph **1**, ^tBu **2**, (4-CH₃)C₆H₄ **3**, (4-C≡CPh)C₆H₄ **4**, (4-CN)C₆H₄ **5**) have been synthesized by reacting [(*p*-cymene)RuCl₂]₂ with the respective alkynylphosphine. Treatment of **1–5** with AgOTf or TIPF₆ and the corresponding PPh₂C≡CR allows the preparation of cationic bis(diphenylphosphino) compounds [(η^6 -*p*-cymene)RuCl(PPh₂C≡CR)₂]⁺X⁻ (X = OTf; R = Ph **6**, ^tBu **7**, (4-CH₃)C₆H₄ **8**, (4-C≡CPh)C₆H₄ **9**, X = PF₆; R = (4-CN)C₆H₄ **10**). All complexes have been characterized by analytical and spectroscopic methods, by cyclic voltammetry, and in several cases (**3** and **7**) by X-ray crystallography. Reactions of both neutral (**1–4**) and cationic (**6–8**) complexes with [*cis*-Pt(C₆F₅)₂(thf)₂] (thf = tetrahydrofuran) gave heterobimetallic neutral [(η^6 -*p*-cymene)Cl-Ru(μ -Cl)(μ -1 κ P: η^2 -PPh₂C≡CR)Pt(C₆F₅)₂] (R = Ph **11a**, ^tBu **12a**, (4-CH₃)C₆H₄ **13a**, (4-C≡CPh)-C₆H₄ **14a**) and cationic [(η^6 -*p*-cymene)(PPh₂C≡CR)Ru(μ -Cl)(μ -1 κ P: η^2 -PPh₂C≡CR)Pt(C₆F₅)₂]⁺(OTf)⁻ (R = Ph **15**, ^tBu **16**, (4-CH₃)C₆H₄ **17**) derivatives stabilized by a mixed Cl/PPh₂C≡CR bridging system. The molecular structures of **12a** and **17** have been confirmed by X-ray diffraction. However, the neutral complexes **11–14** existed in solution as a mixture of isomers [(η^6 -*p*-cymene)ClRu(μ -Cl)(μ -1 κ P: η^2 -PPh₂C≡CR)Pt(C₆F₅)₂] (**a**) and [(η^6 -*p*-cymene)(PPh₂C≡CR)Ru(μ -Cl)₂Pt(C₆F₅)₂] (**b**), respectively.

Introduction

The chemistry of half-sandwich η^6 -arene-ruthenium complexes has been widely developed in the past decade, in part due to their catalytic potential, but also due to their usefulness in the synthesis of other Ru(0) and Ru(II) complexes.^{1–3} In particular, (arene)ruthenium(II) complexes of the type [(η^6 -arene)RuCl₂(PR₃)] containing aryl or alkyl phosphine as ancillary ligands have been extensively studied, owing to their role as effective precursors for a variety of catalytic and stoichiometric organic transformations.^{2,4–9} Special interest is also currently devoted to complexes stabilized by heterobi-

functional phosphines bearing a hard (N, O) donor atom, since these ligands show interesting hemilabile properties.^{10–16} In contrast, the chemistry of analogous (arene)ruthenium(II) complexes containing unsaturated phosphines is relatively unexplored. Recently, Nelson and co-workers have reported (arene)Ru(II) derivatives with vinyl and allyl phosphines and 3,4-dimethyl-1-phenylphosphole, showing interesting reactivity with some of them.^{17,18} Thus, they found that complexes (η^6 -arene)RuCl₂(DPVP)] (DPVP = diphenylvinylphosphine) undergo a novel KO^tBu-promoted hydroalkylation to produce tethered phosphinopropylarene-ruthenium(II) compounds.¹⁹ As far as we are aware, no analogous derivatives have been reported with phosphinoalkynes,

* Corresponding authors. E-mail: elena.lalinde@dq.unirioja.es; forniej@posta.unizar.es.

[†] Universidad de La Rioja, UA-CSIC.

[‡] Universidad de Zaragoza-CSIC.

(1) Bennett, M. A.; Bruce, M. I.; Matheson, T. W. In *Comprehensive Organometallic Chemistry*; Wilkinson, G., Stone, F. G. A., Abel, E. W., Eds.; Pergamon: Oxford, 1982; Vol. 4, p 796.

(2) Le Bozec, H.; Touchard, D.; Dixneuf, P. H. *Adv. Organomet. Chem.* **1989**, *29*, 163.

(3) Bennett, M. A. In *Comprehensive Organometallic Chemistry II*; Abel, E. W., Stone, F. G. A., Wilkinson, G., Eds.; Pergamon: Oxford, 1995; Vol. 7, p 549.

(4) Noyori, R.; Hashiguchi, S. *Acc. Chem. Res.* **1997**, *30*, 97.

(5) Naota, T.; Taka, H.; Murahashi, S. C. *Chem. Rev.* **1998**, *98*, 2599.

(6) Bruneau, C.; Dixneuf, P. H. *Acc. Chem. Res.* **1999**, *32*, 311.

(7) Cadierno, V.; Gamasa, M. P.; Gimeno, J. *Eur. J. Inorg. Chem.* **2001**, 571.

(8) Bruce, M. I. *Chem. Rev.* **1998**, *98*, 2797.

(9) Touchard, D.; Dixneuf, P. H. *Coord. Chem. Rev.* **1998**, *178–180*, 409.

(10) Geldbach, T. J.; Pregosin, P. S. *Eur. J. Inorg. Chem.* **2002**, 1907.

(11) Braunstein, P.; Fryztk, M. D.; Naud, F.; Rettig, S. J. *J. Chem. Soc., Dalton Trans.* **1999**, 589.

(12) Henig, G.; Schulz, M.; Windmüller, B.; Werner, H. *J. Chem. Soc., Dalton Trans.* **2003**, 441.

(13) Cadierno, V.; Diez, J.; García-Garrido, S. E.; García-Granda, S.; Gimeno, J. *J. Chem. Soc., Dalton Trans.* **2002**, 1465, and references therein.

(14) Crochet, P.; Demerseman, B.; Rocaboy, C.; Schleyer, D. *Organometallics* **1996**, *15*, 3084.

(15) Drommi, D.; Arena, C. G.; Nicoló, F.; Bruno, G.; Faraone, F. *J. Organomet. Chem.* **1995**, *485*, 115.

(16) For a recent general (P, N donor ligand) review see: Braunstein, P.; Naud, F. *Angew. Chem., Int. Ed.* **2001**, *40*, 680.

(17) Redwine, K. D.; Hansen, H. D.; Bowley, S.; Isbell, J.; Sánchez, M.; Vodak, D.; Nelson, J. H. *Synth. React. Inorg. Met. Org. Chem.* **2000**, *30*, 379.

(18) Redwine, K. D.; Hansen, H. D.; Bowley, S.; Isbell, J.; Vodak, D.; Nelson, J. H. *Synth. React. Inorg. Met. Org. Chem.* **2000**, *30*, 409.

although these ligands ($\text{PPh}_2\text{C}\equiv\text{CR}$) have revealed an interesting reactivity in transition metal chemistry, such as P–C bond cleavages,^{20–26} insertion,^{27–32} and coupling reactions.^{33,34} In addition, simple P-complexation of these ($\text{Ph}_2\text{PC}_\alpha\equiv\text{C}_\beta\text{-R}$) ligands usually induces a polarization^{35,36} in the alkyne function, with the C_α being partially negatively charged, making them susceptible to electrophilic and nucleophilic reactions with simple molecules such as water,^{37,38} ethanol,^{39,40} XH ,⁴¹ PPh_2H ,⁴² or amines.^{29,32}

In previous papers, when studying the reactivity of [*cis*- $\text{MX}_2(\text{PPh}_2\text{C}\equiv\text{CR})_2$] ($\text{M} = \text{Pd}, \text{Pt}$; $\text{X} = \text{Cl}$,⁴³ C_6F_5 ,^{44,45} or $\text{C}\equiv\text{CR}$;⁴⁶ $\text{R} = \text{Ph}, \text{Tol}, \text{tBu}$; $\text{R}' = \text{Ph}, \text{tBu}$) toward the "*cis*- $\text{Pt}(\text{C}_6\text{F}_5)_2$ " synthon, we have shown an unprecedented and easy chemo-, regio-, and stereoselective insertion of both $\text{PPh}_2\text{C}\equiv\text{CR}$ ligands ($\text{R} = \text{Ph}, \text{Tol}$) into the robust $\text{Pt}-\text{C}_6\text{F}_5$ bond^{44,45} and also the very low η^2 -bonding capability of the bulkier $\text{PPh}_2\text{C}\equiv\text{C}^t\text{Bu}$ ligand.^{43,46,47} Moreover, we have also found that in the iridium species [$\text{Cp}^*\text{IrCl}_2(\text{PPh}_2\text{C}\equiv\text{CPh})$] the phenylethynyl fragment exhibits a stronger η^2 -bonding capability toward $\text{Pt}(\text{II})$ than the analogous rhodium derivative, which is a fact that can be mainly attributed to

the nature of the $\text{M}(\text{M} = \text{Rh}, \text{Ir})-\text{P}$ bond.⁴⁸ As a continuation of our work, we describe in this paper the preparation, characterization, and electrochemical properties of novel neutral [*p*-cymene] $\text{RuCl}_2(\text{PPh}_2\text{C}\equiv\text{CR})$ and cationic [*p*-cymene] $\text{RuCl}(\text{PPh}_2\text{C}\equiv\text{CR})_2^+$ arene complexes, stabilized by different alkynylphosphines. The reactivity of these complexes toward [*cis*- $\text{Pt}(\text{C}_6\text{F}_5)_2(\text{thf})_2$] has been investigated, to gain more insight into the influence of both the $\text{Ru}-\text{P}$ bonds and the nature of the alkynyl substituent in the bonding capability of the alkynyl fragment.

Results and Discussion

(i) Synthesis of Mononuclear Complexes. The novel alkynylphosphines $\text{PPh}_2\text{C}\equiv\text{C}-(4-\text{C}\equiv\text{CPh})\text{C}_6\text{H}_4$ and $\text{PPh}_2\text{C}\equiv\text{C}-(4-\text{CN})\text{C}_6\text{H}_4$, as well as the previously reported $\text{PPh}_2\text{C}\equiv\text{CR}$ ($\text{R} = \text{Ph}$,⁴⁹ tBu ,⁴⁹ $(4-\text{CH}_3)\text{C}_6\text{H}_4$ ⁵⁰) used in this work, have been prepared according to the reported procedure by reaction of chlorodiphenylphosphine with the corresponding lithium acetylide.

The reaction of [$(\eta^6\text{-p-cymene})\text{Ru}(\mu\text{-Cl})\text{Cl}_2$]⁵¹ with 2 molar equiv of alkynylphosphines $\text{PPh}_2\text{C}\equiv\text{CR}$ (Scheme 1, i) in acetone, at room temperature, affords the corresponding mononuclear complexes [$(\eta^6\text{-p-cymene})\text{-RuCl}_2(\text{PPh}_2\text{C}\equiv\text{CR})$] ($\text{R} = \text{Ph}$ **1**, tBu **2**, $(4-\text{CH}_3)\text{C}_6\text{H}_4$ **3**, $(4-\text{C}\equiv\text{CPh})\text{C}_6\text{H}_4$ **4**, $(4-\text{CN})\text{C}_6\text{H}_4$ **5**), which are isolated as air- and moisture-stable orange solids, in moderate (61%) to high (84–94%) yield. As shown in Scheme 1 (path ii), a series of cationic derivatives containing two P-coordinated alkynylphosphines [$(\eta^6\text{-p-cymene})\text{RuCl}(\text{PPh}_2\text{C}\equiv\text{CR})_2$] X ($\text{X} = \text{OTf}$; $\text{R} = \text{Ph}$ **6**, tBu **7**, $(4-\text{CH}_3)\text{-C}_6\text{H}_4$ **8**, $(4-\text{C}\equiv\text{CPh})\text{C}_6\text{H}_4$ **9**, $\text{X} = \text{PF}_6$; $\text{R} = (4-\text{CN})\text{C}_6\text{H}_4$ **10**) were prepared by removing one of the chlorine ligands in the neutral complexes (**1–5**) with silver triflate (**1–4**) or TIPF_6 (**5**) in acetone, followed by subsequent treatment with 1 molar equiv of additional $\text{PPh}_2\text{C}\equiv\text{CR}$. The products were isolated (53–97% yield) by the usual workup (see Experimental Section) as air-stable yellow (**6–9**) or orange (**1–5**, **10**) solids and characterized by means of standard analytic and spectroscopic techniques (see Experimental Section for details), and in the case of complexes [$(\eta^6\text{-p-cymene})\text{-RuCl}_2\{\text{PPh}_2\text{C}\equiv\text{C}(4-\text{CH}_3)\text{C}_6\text{H}_4\}$] (**3**) and [$(\eta^6\text{-p-cymene})\text{-RuCl}(\text{PPh}_2\text{C}\equiv\text{C}^t\text{Bu})_2$](OTf) (**7**), their molecular structures have been confirmed by X-ray crystallography. The IR spectra show a strong or medium (**2**, **4**) $\nu(\text{C}\equiv\text{C})$ band in the 2165–2176 cm^{-1} range, confirming the P-coordination mode of the $\text{PPh}_2\text{C}\equiv\text{CR}$ ligands^{49,50} and, in the case of cationic derivatives, the characteristic absorptions of CF_3SO_3^- or PF_6^- (**10**) anions in the expected regions (see Experimental Section). In all complexes the corresponding phosphorus resonance appears downfield shifted with respect to that of the free $\text{PPh}_2\text{C}\equiv\text{CR}$. As has been previously noted,^{18,52} the chemical shift $\Delta\delta^{31\text{P}}$ is generally greater by 2.15–8.51

(19) Ghebreyessus, K. Y.; Nelson, J. H. *Organometallics* **2000**, *19*, 3387.

(20) Went, M. J. *Polyhedron* **1995**, *14*, 465.

(21) Carty, A. J. *Pure Appl. Chem.* **1982**, *54*, 113, and references therein.

(22) Carty, A. J.; Taylor, N. J.; Smith, W. F. *J. Chem. Soc., Chem. Commun.* **1979**, 750.

(23) Nuccianore, D.; MacLaughlin, S. A.; Taylor, N. J.; Carty, A. J. *Organometallics* **1988**, *7*, 106.

(24) Cherkas, A. A.; Randall, L. H.; MacLaughlin, S. A.; Mott, G. N.; Taylor, N. J.; Carty, A. J. *Organometallics* **1988**, *7*, 969.

(25) Bruce, M. I.; Williams, M. L.; Patrick, J. M.; White, A. H. *J. Chem. Soc., Dalton Trans.* **1985**, 1229.

(26) Hogarth, G.; Rechmond, S. P. *J. Organomet. Chem.* **1997**, *534*, 221.

(27) Bennett, M. A.; Castro, J.; Edwards, A. J.; Kopp, M. R.; Wenger, E.; Willis, A. C. *Organometallics* **2001**, *20*, 980.

(28) Bennett, M. A.; Kwan, L.; Rae, A. D.; Wenger, E.; Willis, A. C. *J. Chem. Soc., Dalton Trans.* **2002**, 226.

(29) Liu, X.; Mok, K. F.; Leung, P. H. *Organometallics* **2001**, *20*, 3918.

(30) Miquel, Y.; Cadierno, V.; Donnadiu, B.; Igau, A.; Majoral, J.-P. *Organometallics* **2000**, *19*, 54.

(31) Dickson, R. S.; de Simone, T.; Parker, R. J.; Fallon, G. D. *Organometallics* **1997**, *16*, 1531.

(32) Liu, X.; Ong, T. K. W.; Selvaratnam, S.; Vittal, J. J.; White, A. J. P.; Williams, D. J.; Leung, P. H. *J. Organomet. Chem.* **2002**, *643*, 4.

(33) Johnson, D. K.; Rukachaisirikul, T.; Y., S.; Taylor, N. J.; Carty, A. J. *Inorg. Chem.* **1993**, *32*, 5544.

(34) Baumgartner, T.; Huynh, K.; Schleidt, S.; Lough, A. J.; Manners, I. *Chem. Eur. J.* **2002**, *8*, 4622.

(35) Louattani, E.; Suades, J. *J. Organomet. Chem.* **2000**, *604*, 234.

(36) Louattani, E.; Suades, J.; Alvarez-Larena, A.; Piniella, F. *Organometallics* **1995**, *14*, 1053.

(37) Jacobson, S. E.; Taylor, N. J.; Carty, A. J. *J. Chem. Soc., Chem. Commun.* **1974**, 668.

(38) Carty, A. J.; Jacobson, S. E.; Simpson, R. T.; Taylor, N. J. *J. Am. Chem. Soc.* **1975**, *97*, 7254.

(39) Restivo, R. J.; Fergusson, G.; Ng, T. W.; Carty, A. J. *Inorg. Chem.* **1977**, *16*, 172.

(40) Bardaji, M.; Laguna, A.; Jones, P. G. *Organometallics* **2001**, *20*, 3906.

(41) Taylor, N. J.; Jacobson, S. E.; Carty, A. J. *Inorg. Chem.* **1975**, *14*, 2648.

(42) Carty, A. J.; Johnson, D. K.; Jacobson, S. E. *J. Am. Chem. Soc.* **1979**, *101*, 5612.

(43) Forniés, J.; Lalinde, E.; Martín, A.; Moreno, M. T.; Welch, A. *J. Chem. Soc., Dalton Trans.* **1995**, 1333.

(44) Charmant, J. P. H.; Forniés, J.; Gómez, J.; Lalinde, E.; Moreno, M. T.; Orpen, A. G.; Solano, S. *Angew. Chem., Int. Ed.* **1999**, *38*, 3058.

(45) Ara, I.; Forniés, J.; García, A.; Gómez, J.; Lalinde, E.; Moreno, M. T. *Chem. Eur. J.* **2002**, *8*, 3698.

(46) Ara, I.; Falvello, L. R.; Fernández, S.; Forniés, J.; Lalinde, E.; Martín, A.; Moreno, M. T. *Organometallics* **1997**, *16*, 5923.

(47) Forniés, J.; García, A.; Gómez, J.; Lalinde, E.; Moreno, M. T. *Organometallics* **2002**, *21*, 3733.

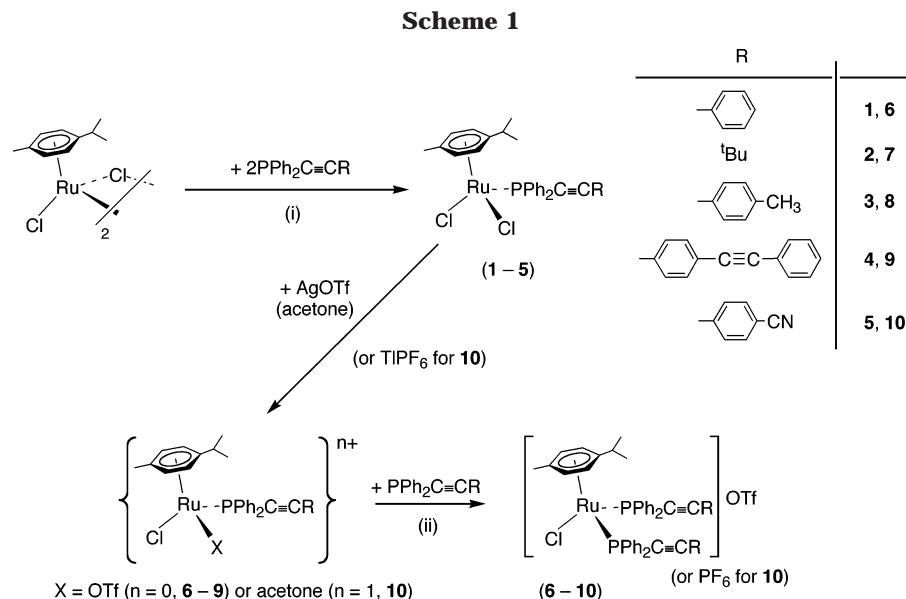
(48) Berenguer, J. R.; Bernechea, M.; Forniés, J.; Gómez, J.; Lalinde, E. *Organometallics* **2002**, *21*, 2314.

(49) Carty, A. J.; Hota, N. K.; Ng, T. W.; Patel, H. A.; O'Connor, T. *J. Can. J. Chem.* **1971**, *49*, 2706.

(50) Louattani, E.; Suades, J.; Mathieu, R. *J. Organomet. Chem.* **1991**, *421*, 335.

(51) Bennett, M. A.; Huang, T.-N.; Matheson, T. W.; Smith, A. K. *Inorg. Synth.* **1982**, *21*, 74.

(52) Valera, P.; Puerta, M. C.; Pandey, D. S. *J. Organomet. Chem.* **2002**, *648*, 27.

**Table 1. Crystallographic Data for 3, 7, 12a·(CH₃)₂CO, and 17·2CHCl₃**

	3	7	12a·(CH₃)₂CO	17·2CHCl₃
empirical formula	C ₃₁ H ₃₁ Cl ₂ PRu	C ₄₇ H ₅₂ ClF ₃ O ₃ P ₂ RuS	C ₄₃ H ₃₉ Cl ₂ F ₁₀ OPPtRu	C ₆₇ H ₅₀ Cl ₇ F ₁₃ O ₃ P ₂ PtRuS
fw	606.50	952.41	1159.77	1788.38
temperature (K)	173(1)	223(1)	173(1)	223(1)
cryst syst	triclinic	orthorhombic	orthorhombic	triclinic
space group	<i>P</i> $\bar{1}$	<i>Pc</i> 2 ₁ n	<i>P</i> 2 ₁ 2 ₁ 2 ₁	<i>P</i> $\bar{1}$
<i>a</i> (Å)	9.3190(2)	15.5177(2)	12.9120(2)	12.3570(1)
<i>b</i> (Å)	11.7550(2)	16.8310(3)	14.1900(2)	14.3450(2)
<i>c</i> (Å)	12.9270(3)	17.4242(3)	23.1560(5)	19.7060(3)
α (deg)	94.2310(10)	90	90	90.2420(10)
β (deg)	100.5360(10)	90	90	91.8630(10)
γ (deg)	99.1860(10)	90	90	103.8720(10)
volume (Å ³)	1366.60(5)	4550.82(13)	4242.67(13)	3389.17(8)
<i>Z</i>	2	4	4	2
<i>D</i> _{calcd} (Mg/m ³)	1.474	1.390	1.816	1.752
abs coeff (mm ⁻¹)	0.846	0.571	3.891	2.721
<i>F</i> (000)	620	1968	2264	1760
cryst size (mm)	0.40 × 0.30 × 0.15	0.40 × 0.30 × 0.30	0.30 × 0.25 × 0.12	0.35 × 0.25 × 0.25
θ range for data collection (deg)	1.61 to 27.97	4.11 to 27.56	3.00 to 25.68	4.14 to 27.88
no. of data/restraints/params	6485/0/320	10100/7/533	7949/4/540	15974/18/897
goodness-of-fit on <i>F</i> ²	1.027	1.031	1.031	1.035
final <i>R</i> indices [<i>I</i> > 2 σ (<i>I</i>)]	<i>R</i> ₁ = 0.0320, <i>wR</i> ₂ = 0.0709	<i>R</i> ₁ = 0.0448, <i>wR</i> ₂ = 0.1034	<i>R</i> ₁ = 0.0371, <i>wR</i> ₂ = 0.0757	<i>R</i> ₁ = 0.0434, <i>wR</i> ₂ = 0.0970
<i>R</i> indices (all data)	<i>R</i> ₁ = 0.0457, <i>wR</i> ₂ = 0.0752	<i>R</i> ₁ = 0.0694, <i>wR</i> ₂ = 0.1137	<i>R</i> ₁ = 0.0468, <i>wR</i> ₂ = 0.0788	<i>R</i> ₁ = 0.0687, <i>wR</i> ₂ = 0.1071
largest diff peak and hole (e ⁻ Å ⁻³)	0.576 and -0.716	0.599 and -0.806	1.575 and -0.846	0.909 and -1.297

ppm for the cationic $[(\eta^6\text{-}p\text{-cymene})\text{RuCl}(\text{PPh}_2\text{C}\equiv\text{CR})_2]\text{X}$ (**6–10**) complexes ($\Delta\delta$ 36.79–40.22 ppm) than for the neutral (**1–5**) derivatives ($\Delta\delta$ 30.30–34.64 ppm). It is remarkable that for the neutral complexes the observed $\Delta\delta$ increases (**2** < **3** < **1** < **4** < **5**) as the acceptor properties of the C \equiv CR ligands increase (R = ^tBu < (4-CH₃)C₆H₄ < Ph < (4-C \equiv CPh)C₆H₄ < (4-CN)C₆H₄). When the uncoordinated P-C α and C β alkyne carbon resonances^{35,36,47,48} are compared with those of the free phosphines, several trends are clearly observed: Upon coordination, the C α resonances (doublet in **1–5**, or A part of an AXX' spin system in **6–9**) shift upfield, this shift, $\Delta\delta$ (ppm), being particularly significant in the cationic derivatives ($\Delta\delta$ 1.6–3.7 ppm for **1–5** vs 4.8–9.8 ppm for **6–9**). On the other hand, and in accordance with previous observations,⁴⁸ in Rh and Ir(III) derivatives, the C β signals are only slightly affected in the neutral complexes (**1–5**), but clearly move downfield for the cationic ones (Δ 3.8 **6**, 3.3 **7**, 6.0 **8**, 5.3 **9** ppm). As a consequence, the final chemical shift differences (δC_{β} –

δC_{α}), which are related to the polarization of the C \equiv C triple bond, are notably higher in the cationic bis-(phosphine)ruthenium complexes than in the neutral $[(\eta^6\text{-}p\text{-cymene})\text{RuCl}_2(\text{PPh}_2\text{C}\equiv\text{CR})]$ derivatives. Interestingly, we had previously observed that complexation of two PPh₂C \equiv CR molecules to the neutral "Ru(η^5 -C₅-Me₅)Cl" fragment does not have an effect on the alkyne polarization.⁴⁸ The steric constraint around the metal center in the cationic **6–9** derivatives containing two PPh₂C \equiv CR ligands is clearly reflected in the ¹³C signals due to the phenyl rings bonded to phosphorus, which are chemical shift inequivalent, thus suggesting that the rotation across the Ru–P bond is hindered or at least slow on the NMR time scale.

X-ray crystallographic analyses confirm the structures of **3** and **7** (Table 1 and Figure 1). Both the neutral derivative **1** and the cation **7**⁺ exhibit the expected and usual pseudo-octahedral half-sandwich disposition around the Ru atom, with the *p*-cymene ligand occupying one face of the octahedron. The Ru–Cl distance, slightly

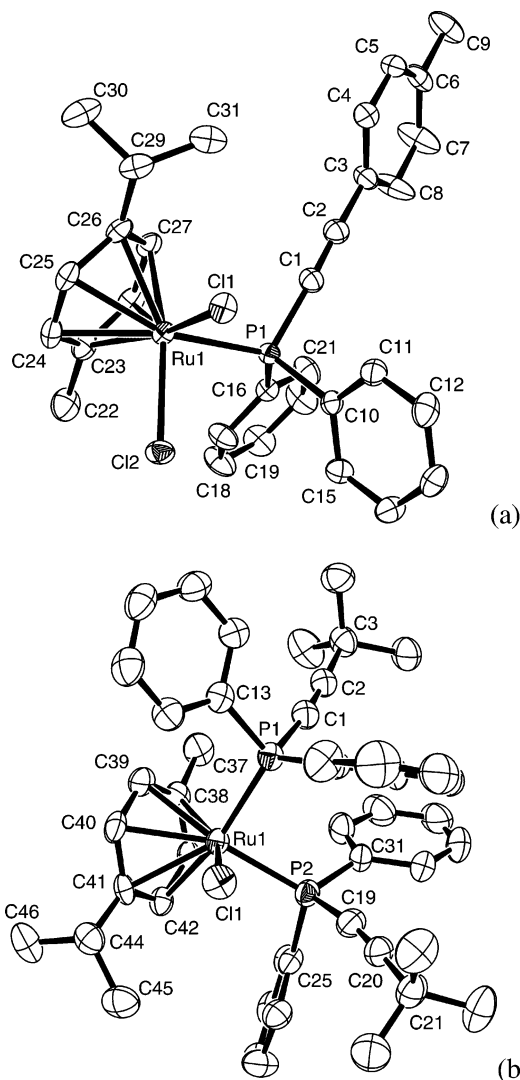


Figure 1. Molecular structure of (a) $[(\eta^6\text{-}p\text{-cymene})\text{RuCl}_2\text{-PPh}_2\text{C}\equiv\text{C}(4\text{-CH}_3)\text{C}_6\text{H}_4]$, **3**, and (b) the cation $[(\eta^6\text{-}p\text{-cymene})\text{RuCl}(\text{PPh}_2\text{C}\equiv\text{C}^t\text{Bu})_2]^+$ in **7**. Selected bond lengths (Å) and angles (deg): **3**: Ru–P 2.3289(6), Ru–Cl 2.4024(6), 2.4109(6), P–C $_{\alpha}$ 1.760(2), C $_{\alpha}$ –C $_{\beta}$ 1.198(3), P–Ru–Cl 84.73(2), 86.97(2), Cl–Ru–Cl 88.37(2), P–C $_{\alpha}$ –C $_{\beta}$ 173.0(2), C $_{\alpha}$ –C $_{\beta}$ –C $_{\gamma}$ 174.7(2); **7**: Ru–P 2.3278(12), 2.3451(11), Ru–Cl 2.3849(11), P–C $_{\alpha}$ 1.748(5), 1.745(5) C $_{\alpha}$ –C $_{\beta}$ 1.196(6), 1.187(6), P–Ru–Cl 85.96(4), 88.89(4), P–Ru–P 91.64(4), P–C $_{\alpha}$ –C $_{\beta}$ 172.9(4), 171.7(4), C $_{\alpha}$ –C $_{\beta}$ –C $_{\gamma}$ 176.2(5), 176.7(5).

shorter in **7**⁺ (2.3849(11) Å) than those observed in **3** (2.4024(6), 2.4109(6) Å), Ru–P lengths (2.3289(6) Å **3**; 2.3278(12), 2.3451(11) Å in **7**⁺), and the P–Ru–Cl and/or P–Ru–P and Cl–Ru–Cl angles are unexceptional for (arene)rutheniumchlorophosphine derivatives.^{17,18,53} The Ru–C distances are slightly longer in the cation (range for **7**⁺ 2.222(4)–2.312(4) Å) than in the neutral complex (range for **3** 2.168(2)–2.244(2) Å), but compare well with the values found in related cationic or neutral Ru(II)-*p*-cymene complexes. The neutral complex **3** shows a clear $\eta^4\text{-}\eta^2$ distortion, with two short bonds (Ru–C(28) 2.168(2) Å, Ru–C(27) 2.179(2) Å) *trans* to the Ru–P bond and four longer bonds (2.216(2)–2.244(2) Å) *trans* to the Ru–Cl bonds. This finding reflects the higher *trans* influence of the phosphorus ligands and

has been previously observed for related $(\text{arene})(\text{PR}_3)\text{-Ru}^{\text{II}}\text{L}_2$ complexes.^{53,54}

The uncoordinated alkynyl fragments in the phosphine ligands in both species display a virtually linear geometry, with typical C≡C bond distances (1.187(6)–1.198(3) Å). It should be mentioned that the two acetylene units in the cation **7**⁺ do not exhibit the eclipsed arrangement previously found in $[\text{Cp}^*\text{MCl}(\text{PPh}_2\text{C}\equiv\text{CPh})_2]^+$ (M = Rh, Ir) and $[\text{Cp}^*\text{RuCl}(\text{PPh}_2\text{C}\equiv\text{CPh})_2]^+$,⁴⁸ containing the diphenyl(phenylethynyl)phosphine. As is observed in Figure 1b, in the cation $[(\eta^6\text{-}p\text{-cymene})\text{RuCl}(\text{PPh}_2\text{C}\equiv\text{C}^t\text{Bu})_2]^+$ and, probably, because of the presence of two P-bonded bulkier *tert*-butylalkynylphosphines, the torsion angle C $_{\alpha}$ –P–P–C $_{\alpha}$ is 119.7°.

The electrochemistry of the complexes was investigated by cyclic voltammetry (see Experimental Section for details). For the neutral complexes **1**–**5**, chemically reversible one-electron Ru(II)/Ru(III) oxidations were observed with potentials ranging from 0.69 to 0.74 V, following correlation **2** < **3** < **1** < **4** < **5** identical to that observed with $\Delta\delta^{31}\text{P}$, i.e., $\Delta\delta^{31}\text{P}$ increases as $E_{1/2}$ increases. Probably, due to their cationic nature, complexes **9** and **10** do not give electrochemical response between the CH_2Cl_2 windows. However, complexes **6**–**8** show no response from 0 to 1.8 V, but they unexpectedly exhibit an irreversible reduction wave between –1.590 and –1.685 V, followed of a small oxidation feature between –1.022 and –1.111 V in the reverse scan (all values vs Fe^+/Fe).

(ii) Synthesis of Heterobinuclear Complexes.

During the past decades important efforts have been made to synthesize structurally defined polynuclear complexes, in particular, heterobinuclear complexes, mainly due to their potential application in catalysis.^{55–58} We have previously shown that $[\text{cis-Pt}(\text{C}_6\text{F}_5)_2(\text{thf})_2]$ (thf = tetrahydrofuran), having two weakly coordinating tetrahydrofuran molecules, is an excellent precursor to homo- and heterobimetallic systems containing the *cis*-Pt(C $_6$ F $_5$) $_2$ moiety.^{43,46–48,59–62} To examine the bonding capability of the alkynyl fragments in the neutral (**1**–**5**) and cationic (**6**–**10**) ruthenium(alkynylphosphine κ -P) complexes, the study of their reactivity toward $[\text{cis-Pt}(\text{C}_6\text{F}_5)_2(\text{thf})_2]$ was undertaken. The results of this study are shown in Scheme 2.

At room temperature, the neutral compounds **1**–**4** react with $[\text{cis-Pt}(\text{C}_6\text{F}_5)_2(\text{thf})_2]$ in CH_2Cl_2 to yield $[(\eta^6\text{-}p\text{-cymene})\text{ClRu}(\mu\text{-Cl})(\mu\text{-}1\kappa\text{P}:\eta^2\text{-PPh}_2\text{C}\equiv\text{CR})\text{Pt}(\text{C}_6\text{F}_5)_2]$ (**11a**–**14a**) as red (**11a**, **13a**), salmon pink (**12a**), or brown (**14a**) solids. It should be noted that the analogous reaction between $[(\eta^6\text{-}p\text{-cymene})\text{RuCl}_2\{\text{PPh}_2\text{C}\equiv\text{C}(4\text{-CN})\text{C}_6\text{H}_4\}]$ (**5**) and $[\text{cis-Pt}(\text{C}_6\text{F}_5)_2(\text{thf})_2]$ yields only a complex mixture of products, from which no pure compound could be separated. Although two isomers are possible, the IR spectra and the examination of several crystals of **12a** by X-ray spectroscopy revealed the presence of only one isomer in the solid state, the one stabilized by a mixed $(\mu\text{-Cl})(\mu\text{-}\kappa\text{P}:\eta^2\text{-PPh}_2\text{C}\equiv\text{CR})$ bridging system. Complexes **11a**–**14a** have been fully char-

(54) Smith, P. D.; Gelbrich, T.; Hursthouse, M. B. *J. Organomet. Chem.* **2002**, *659*, 1.

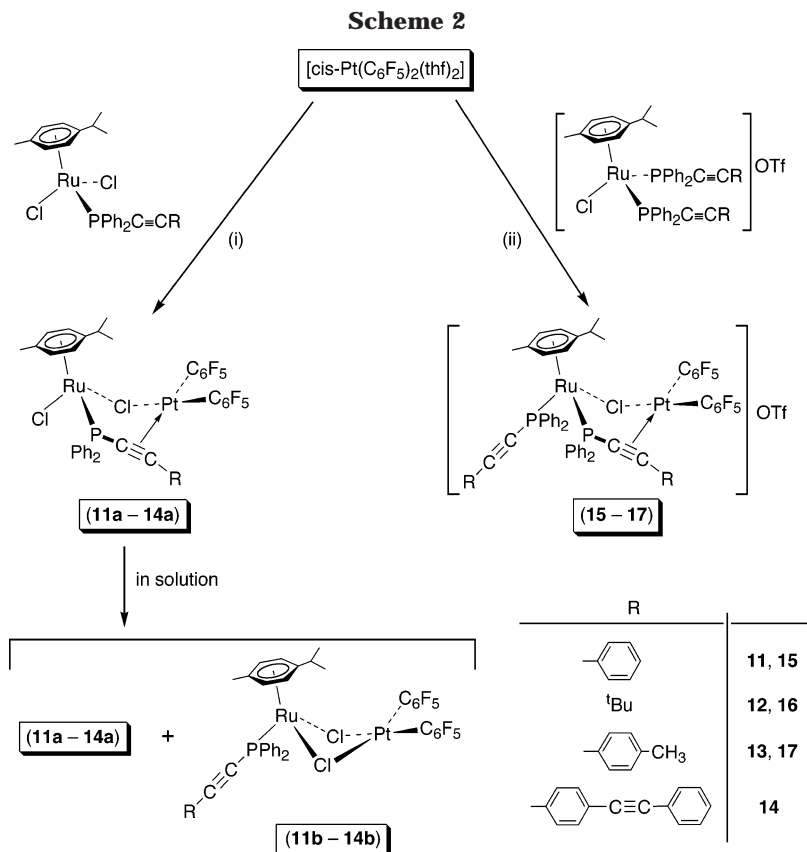
(55) Severin, K. *Chem. Eur. J.* **2002**, *8*, 1515.

(56) Wheatley, P.; Kalck, P. *Chem. Rev.* **1999**, *99*, 3379.

(57) Stephan, W.; Nadasdi, T. T. *Coord. Chem. Rev.* **1996**, *147*, 147.

(58) Adams, R. D. In *Comprehensive Organometallic Chemistry II*; Wilkinson, G., Stone, F. G. A., Abel, E. W., Eds.; Pergamon: Oxford, 1995; Vol. 10, p 1.

(53) Pinto, P.; Marconi, G.; Heinemann, F. W.; Zenneck, U. *Organometallics* **2004**, *23*, 374.



acterized by elemental analyses, IR, $^{31}\text{P}\{^1\text{H}\}$, and ^{19}F NMR spectroscopy, mass spectrometry ES(+), and, in the case of **12a**, X-ray diffraction methods. Thus, the IR spectra of complexes **11a–13a** exhibit only a medium-intensity $\nu(\text{C}\equiv\text{C})$ band at ca. 1990 cm^{-1} (1989 **11**; 1990 **12**, 1987 cm^{-1} **13**), typical of bridging $\mu\text{-PPh}_2\text{C}\equiv\text{CR}$ ligands.^{43,46–48} As expected, complex **14a**, containing the $\text{C}\equiv\text{C}-\text{C}_6\text{H}_4-\text{C}\equiv\text{C}-\text{Ph}$ diynyl fragment, shows the presence of free (2170 cm^{-1}) and bridging (1965 cm^{-1}) $\text{C}\equiv\text{C}$ alkynyl units.

In addition, we obtained crystals of **12a**, which were suitable for single-crystal X-ray diffraction analysis, and examination of several crystals, as we have noted, revealed the presence of only one isomer, the mixed ($\mu\text{-Cl})(\mu\text{-}\kappa\text{P},\eta^2\text{-PPh}_2\text{C}\equiv\text{CR})$ bridged form. Complex **12a** crystallizes in the chiral space group $P2_12_12_1$, with four symmetry-related molecules of only one enantiomer at the ruthenium center (*S*) and four acetone solvent molecules in the unit cell. We noted that the crystal structure of another crystal chosen from the same sample gives the same structure, but showing an absolute configuration *R* at the Ru, thus indicating that both enantiomers are present in the crystalline mixture. The molecular structure of **12a** is presented in Figure 2, and selected bond lengths and angles are given in Table 2. It is noteworthy that, despite the presence of two chloride ligands in the precursor, in the final binuclear compound the organometallic ruthenium fragment has a preference in the solid state to act as a mixed $\text{Cl},\eta^2(\text{alkyne})$ bidentate ligand toward the " $\text{cis-Pt}(\text{C}_6\text{F}_5)_2$ " entity. The ruthenium atom presents the typical piano-stool geometry, with the *p*-cymene ligand coordinated in the usual η^6 -mode, and the platinum center has the expected square-planar geometry. The Ru(1)–Cl(1) bridging distance ($2.4413(16)\text{ \AA}$) is slightly longer than

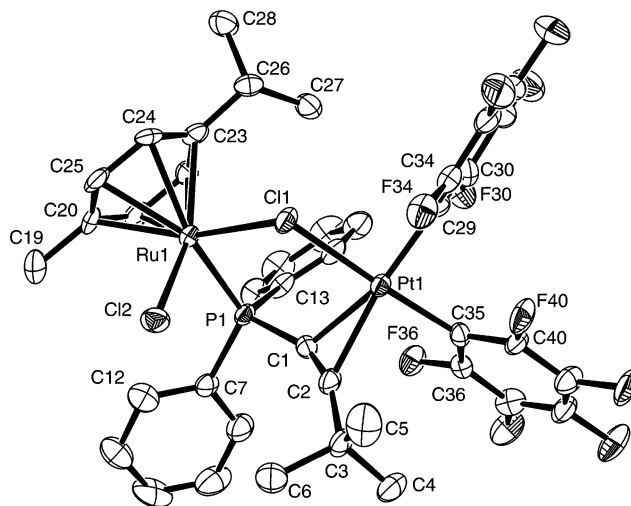


Figure 2. ORTEP view of $[(\eta^6\text{-}p\text{-cymene})\text{ClRu}(\mu\text{-Cl})(\mu\text{-}\kappa\text{P},\eta^2\text{-PPh}_2\text{C}\equiv\text{C}^t\text{Bu})\text{Pt}(\text{C}_6\text{F}_5)_2]$, **12a**. Ellipsoids are drawn at the 50% probability level. Hydrogen atoms have been omitted for clarity.

the terminal Ru(1)–Cl(2) ($2.3941(18)\text{ \AA}$) bond length and comparable to that previously found in $[(\text{PPh}_2\text{C}\equiv\text{CPh})\text{-Cp}^*\text{Ru}(\mu\text{-Cl})(\mu\text{-}\kappa\text{P},\eta^2\text{-PPh}_2\text{C}\equiv\text{CPh})\text{Pt}(\text{C}_6\text{F}_5)_2]$, **A**.⁴⁸ The Pt–Cl ($2.4116(15)\text{ \AA}$) and $\eta^2\text{-Pt-C}(1),\text{C}(2)$ acetylenic ($2.177(6)$, $2.218(7)\text{ \AA}$) bond distances are very close to those found in **A** (Pt–Cl $2.3785(9)\text{ \AA}$; Pt–C(acetylenic) $2.229(3)$, $2.226(4)\text{ \AA}$). However, the degree of folding of the *tert*-butylethynyl portion in the phosphine ligand caused by coordination to the Pt atoms was found to be significantly greater than that seen in the phenylethynyl fragment in complex **A** (angles at C(1) and C(2), $155.1(6)^\circ$ and $159.2(2)^\circ$ in **12a** vs 162.3° and 166.3° in **A**). The Ru–Pt separation, 4.121 \AA , consistent with the

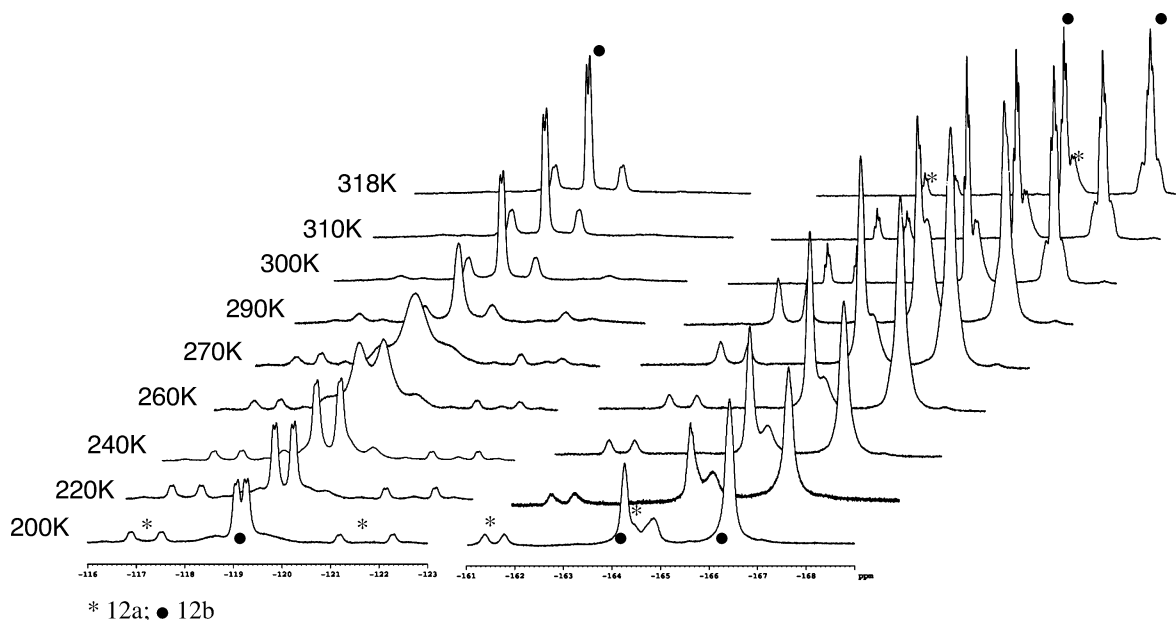


Figure 3. Variable-temperature ^{19}F NMR spectra of **12** (**12a** (*) + **12b** (●), $\text{R} = \text{tBu}$) in CD_3COCD_3 .

Table 2. Selected Bond Lengths [Å] and Angles [deg] for $[(\eta^6\text{-}p\text{-cymene})\text{ClRu}(\mu\text{-Cl})\text{-}(\mu\text{-}1\kappa\text{P}\text{-}\eta^2\text{-PPh}_2\text{C}\equiv\text{C}^t\text{Bu})\text{Pt}(\text{C}_6\text{F}_5)_2]\cdot(\text{acetone})$ (12a**·acetone) and $[(\eta^6\text{-}p\text{-cymene})(\text{PPh}_2\text{C}\equiv\text{CTol})\text{Ru}(\mu\text{-Cl})\text{-}(\mu\text{-}1\kappa\text{P}\text{-}\eta^2\text{-PPh}_2\text{C}\equiv\text{CTol})\text{Pt}(\text{C}_6\text{F}_5)_2](\text{OTf})\cdot 2\text{CHCl}_3$ (**17**· 2CHCl_3)**

	12a · $(\text{CH}_3)_2\text{CO}$	17 · 2CHCl_3
Pt–C _{ipso} (C ₆ F ₅)	2.033(7)	2.030(4)
Pt–Cl	2.023(6)	2.025(4)
Pt–C _α	2.4116(15)	2.4081(9)
Pt–C _β	2.177(6)	2.188(4)
Pt–C _γ	2.218(7)	2.229(4)
Ru– $\eta^6\text{-C}$ (arene)	2.167(7)–2.246(6)	2.236(4)–2.328(4)
Ru–P _(b)	2.3194(18)	2.3390(10)
Ru–P _(t)		2.3346(11)
Ru–Cl _(b)	2.4413(16)	2.4140(11)
Ru–Cl _(t)	2.3941(18)	
P–C _α (b)	1.766(6)	1.782(5)
P–C _α (t)		1.745(5)
C _α –C _β (b)	1.199(9)	1.241(6)
C _α –C _β (t)		1.191(6)
Pt–Ru	4.121	4.094
C _{ipso} (C ₆ F ₅)–Pt–C _{ipso} (C ₆ F ₅)	90.1(3)	87.88(17)
cis Cl–Pt–C _{ipso} (C ₆ F ₅)	87.39(17)	89.87(11)
cis C _α –Pt–C _{ipso} (C ₆ F ₅)	99.2(3)	100.96(16)
cis C _β –Pt–C _{ipso} (C ₆ F ₅)	86.0(3)	85.20(16)
C _α –Pt–C _β	31.6(2)	32.63(15)
Cl–Pt–C _α	83.28(17)	81.89(11)
Cl–Pt–C _β	96.39(18)	96.12(10)
P _(b) –Ru–Cl _(b)	88.26(6)	87.48(4)
P–Ru–Cl	87.11(6)	89.03(4)
Cl–Ru–Cl	85.81(6)	
P–Ru–P		94.01(4)
Ru–Cl–Pt	116.27(7)	116.22(4)
P–C _α –C _β (b)	155.1(6)	159.4(4)
P–C _α –C _β (t)		175.0(4)
C _α –C _β –C _γ (b)	159.2(7)	166.0(4)
C _α –C _β –C _γ (t)		179.0(5)

open Ru(1)–Cl(1)–Pt(1) angle (116.27(7)°), excludes any direct intermetallic interaction.

Notwithstanding, the ^1H , $^{31}\text{P}\{^1\text{H}\}$, and ^{19}F NMR spectroscopy clearly showed the presence of two species at room temperature in a ca. 55–60:45–40 proportion in CDCl_3 and ca. 25–30:75–70 in acetone- d_6 , suggesting that both of the possible isomers $[(\eta^6\text{-}p\text{-cymene})\text{ClRu}(\mu\text{-Cl})(\mu\text{-}1\kappa\text{P}\text{-}\eta^2\text{-PPh}_2\text{C}\equiv\text{CR})\text{Pt}(\text{C}_6\text{F}_5)_2]$ (**a**) and $[(\eta^6\text{-}p\text{-}$

cymene)($\text{PPh}_2\text{C}\equiv\text{CR})\text{Ru}(\mu\text{-Cl})_2\text{Pt}(\text{C}_6\text{F}_5)_2]$ (**b**) were present in solution. The presence of both isomers in solution, but only one in the solid state, suggests the occurrence of crystallization-induced transformation, probably due to steric reasons in the lattice. In the $^{31}\text{P}\{^1\text{H}\}$ NMR spectra, two singlets corresponding to both isomers appeared. The resonance that appears significantly low field shifted ($\delta(\text{P})$ 46.32–48.55) with respect to the corresponding precursor is attributed to the bridging phosphine ligand in the isomer **a**. Similar downfield shifts ($\Delta(\delta\text{P})$) from 47.88 ppm for **14a** to 55.49 ppm for **12a** have been previously observed in other complexes containing $\mu\text{-}\kappa\text{P}\text{-}\eta^2\text{-PPh}_2\text{C}\equiv\text{CR}$ ligands, this being attributed to the loss of the electron ring current upon complexation.^{46–48} The less deshielded signal, which in each case appears relatively close to the corresponding one in the precursor, is attributed to the minor isomer in CDCl_3 ($\delta(\text{P})$ 7.10–9.80) stabilized by chloride bridges. Variable-temperature ^1H and ^{19}F NMR spectra indicate a temperature dependence of the spectral patterns and also of the molar ratio between the isomers, the mixed bridged form **a** increasing as the temperature is lowered. It should be noted that complex **12a** is only sparingly soluble in CDCl_3 (enough for a ^1H NMR spectrum), and the ^{19}F NMR spectra were recorded in acetone- d_6 . In this solvent the ratio **12a**:**12b** is nearly temperature independent, being ~30:70 at 200 K, which is similar to that observed at 293 K. In all complexes, the presence of separated patterns for both isomers, even at high temperature, indicates that their interconversion is slow on the NMR time scale. To illustrate this, the temperature dependence of the ^{19}F NMR spectra of **12** in $\text{CD}_3\text{-COCD}_3$ and of the ^1H NMR spectra for **13** in CDCl_3 are shown in Figures 3 and 4. As can be observed, the limiting low-temperature ^{19}F spectrum of **12** shows a pattern compatible with a static structure for both isomers, indicating that the rotation of C_6F_5 groups about the Pt–C bond is hindered. In all complexes studied, the signals due to *m*-fluorine atoms appear partially overlapped or are coincident. Upon raising the temperature, the rotation of C_6F_5 rings becomes rapid

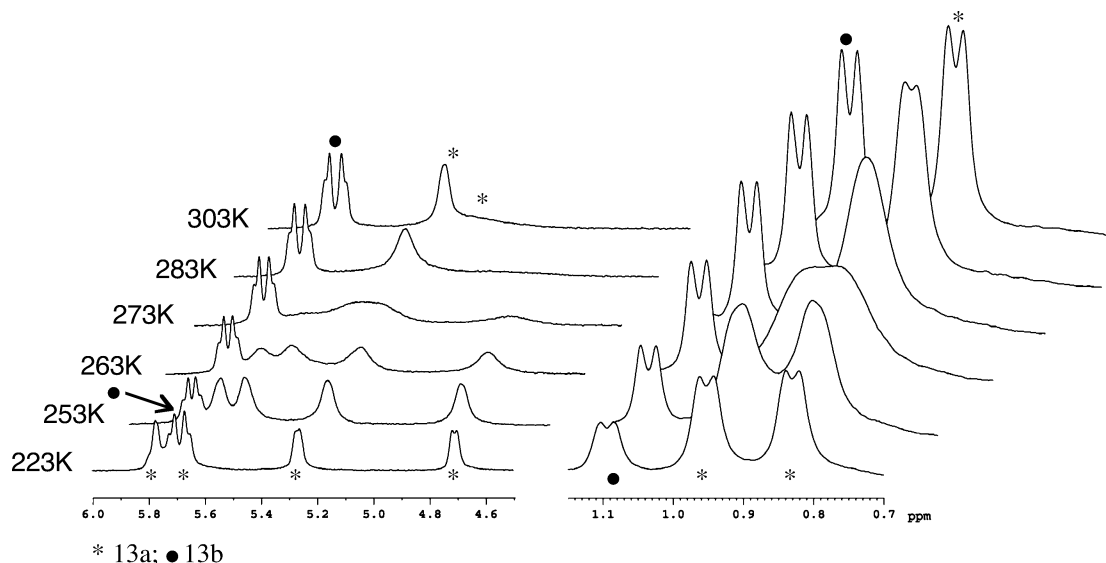


Figure 4. Variable-temperature ^1H NMR spectra in a selected region (C_6H_4 and CHMe_2 , *p*-Cy) of **13** (**13a** (*) + **13b** (●)), $\text{R} = (4\text{-CH}_3)\text{C}_6\text{H}_4$) in CDCl_3 .

in the two isomers. Based on the coalescence of the *o*-fluorine signals, the calculated energy barriers are $\Delta G_{270}^\ddagger \approx 54 \text{ kJ}\cdot\text{mol}^{-1}$ for **12b**, $\Delta G_{290}^\ddagger \approx 51 \text{ kJ}\cdot\text{mol}^{-1}$ and $\Delta G_{318}^\ddagger \approx 57 \text{ kJ}\cdot\text{mol}^{-1}$ for **12a**. The behavior of the other complexes is similar, but the NMR spectra were recorded in CDCl_3 , and in this solvent at low temperature the major isomer observed is the mixed bridged (238 K; for **11a:11b** and **14a:14b** 75:25 and for **13a:13b** 80:20, see Experimental Section for details).

The ^1H NMR resonances of the doubly chloride-bridged species **11b–14b** are unexceptional and, as expected, do not change appreciably with the temperature. On the contrary, in the mixed bridged isomers **11a–14a**, in which coordination of only one of the two chloride ligands creates chirality at the ruthenium center, the expected nonequivalence of the two halves of the *p*-cymene ligands was only distinguishable at room temperature for the *tert*-butylethynylphosphine derivative **12a** and for the remaining complexes at low temperature. As can be observed in Figure 4, which shows a section of the temperature dependence of the ^1H spectra for **13**, at 293 K only two arene (C_6H_4) and one methyl (d, $\text{CH}(\text{CH}_3)_2$) resonances are seen for the *p*-cymene ligand in the isomer **13a**; the CH singlet at ca. 5.2 ppm was extremely broad, suggesting that this temperature was close to the coalescence point. By lowering the temperature, the ratio **13a:13b** increases and the CH (C_6H_4) and Me ($\text{CH}(\text{CH}_3)_2$) resonances broaden, collapse, and, finally, split. At the low-exchange limit, all four arene-ring protons and the two methyl groups of the CHMe_2 entity became inequivalent. The latter give rise to two different doublets (δ 0.95, 0.83) with identical integrated intensities. In this complex (**13a**), the coalescence temperature for the methyl resonances and for the CH signals located at 4.71 and 5.78 ppm were measured at 263 and 288 K, respectively, both data treatments yielding an energy barrier of ca. $54 \text{ kJ}\cdot\text{mol}^{-1}$. Similar barriers were measured for complexes **11a** ($\approx 53.8 \text{ kJ}\cdot\text{mol}^{-1}$) and **14a** (53.9 (Me) and 54.5 (CH) $\text{kJ}\cdot\text{mol}^{-1}$). As the two C_6F_5 rings are nonequivalent even at high temperature, the observed equilibration of the two halves of the *p*-cymene ligand is probably caused by a fast rupture of the Pt–

Cl, followed by a reorientation of the *cis*-Pt(C_6F_5) $_2(\eta^2$ -alkyne) unit, and bonding to the other chlorine ligand. Despite the presence of mixtures of binuclear species **11a–14a/11b–14b**, the cyclic voltammograms of these complexes in CH_2Cl_2 exhibit only an irreversible oxidation wave in the narrow range from 1.17 to 1.26 V. In each case, the wave is attributed to the RuII/III couple, being significantly positively shifted ($\Delta(\text{mV})$ 483 **11**, 480 **12**, 420 **13**, 478 **14**) compared to that of the corresponding neutral precursor (**1–4**), which is consistent with electron donation through the bridging ligand (Cl or phosphine) to the more electron-deficient Pt center.

As shown in Scheme 2 (ii), treatment of the bis-(diphenyl)ethynylphosphine cationic derivatives **6–8** with [*cis*-Pt(C_6F_5) $_2(\text{thf})_2$] in CH_2Cl_2 yielded cationic heterobridged heterobimetallic complexes [$(\eta^6$ -*p*-cymene)(PPh $_2\text{C}\equiv\text{CR})\text{Ru}(\mu\text{-Cl})(\mu\text{-1}\kappa\text{P}:\eta^2\text{-PPh}_2\text{C}\equiv\text{CR})\text{Pt}(\text{C}_6\text{F}_5)_2(\text{OTf})$] ($\text{R} = \text{Ph}$ **15**, tBu **16**, $(4\text{-CH}_3)\text{C}_6\text{H}_4$ **17**), which are isolated as air-stable yellow solids in high yields (71–95%). All attempts to obtain analogous bimetallic complexes under similar reaction conditions starting from **9** and **10** were fruitless. Complexes **15–17**, whose acetone solutions behave as the expected 1:1 electrolytes, have been characterized by usual spectroscopic techniques and, in the case of the tolylethynyl derivative complex **17**, its structure confirmed by an X-ray diffraction study. Their IR spectra confirm the presence of bridging ($\nu(\text{C}\equiv\text{CR})$ 1988 **15**, 1977 **16**, and 1972 cm^{-1} **17**) and terminal ($\nu(\text{C}\equiv\text{C})$ 2168 **15**, 2165 **16**, and 2170 cm^{-1} **17**) PPh $_2\text{C}\equiv\text{CR}$ ligands. The $^{31}\text{P}\{^1\text{H}\}$ NMR spectra also confirm the inequivalence of both phosphine ligands displaying two doublets in the range 36.51–51.55 ppm and 0.72–2.98 ppm ($^2J_{\text{P-P}}$ 53 Hz **15**, **17** and 51 Hz **16**), respectively. The low-field signal, which is strongly deshielding in relation to the corresponding precursor, is attributed, as in isomers **11a–14a**, to the bridging phosphine ligand, and the high-field resonance, which appears close to those seen in the precursors, is assigned to the terminal P-coordinated ligand. Due to the chirality of the formed binuclear derivatives, all four arene ring protons and the methyl groups of the CHMe_2 entity in the *p*-cymene ligand became inequivalent. As expected, the latter give rise to two different doublets in

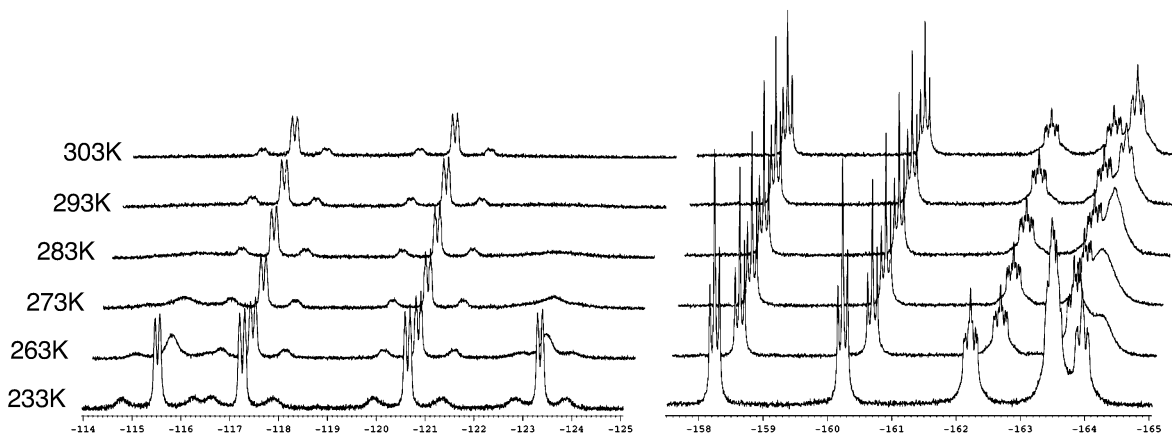


Figure 5. Variable-temperature ^{19}F NMR spectra of $[(\eta^6\text{-}p\text{-cymene})\{\text{PPh}_2\text{C}\equiv\text{C}(4\text{-CH}_3)\text{C}_6\text{H}_4\}\text{Ru}(\mu\text{-Cl})\mu\text{-}1\kappa\text{P}:\eta^2\text{-PPh}_2\text{C}\equiv\text{C}(4\text{-CH}_3)\text{C}_6\text{H}_4\}\text{Pt}(\text{C}_6\text{F}_5)_2](\text{OTf})$, **17**, in CDCl_3 .

their ^1H spectra with identical intensities in the spectroscopic range 0.98–1.1 ppm.

The temperature dependence of the ^{19}F NMR spectra of complexes **15** and **17** is similar. In both complexes, the rotation of one C_6F_5 group around the $\text{Pt}-i\text{-C}$ bond is hindered over all the range of temperatures studied (-40 to 40 $^\circ\text{C}$), while the energy barrier for the other is lower, being static only at low temperature, as is clearly seen in Figure 5 for complex **17** (see Experimental Section for details). The free energy of activation ΔG^\ddagger for the dynamic ring calculated, using the *ortho* and *meta* fluorine resonances, is 51.7 ± 0.1 $\text{kJ}\cdot\text{mol}^{-1}$ in complex **17** and 52.5 ± 0.1 $\text{kJ}\cdot\text{mol}^{-1}$ in complex **15**. The dynamic behavior observed for one ring is tentatively ascribed to the less sterically hindered C_6F_5 group mutually *cis* to the $\mu\text{-Cl}$ bridging group. We noted that the rotation of this ring could be more easily achieved, due to the fact that it is located *trans* to the η^2 -acetylenic entity, which is known to have a higher *trans*-influence than the chlorine group. In the *tert*-butylethynylphosphine complex **16**, both C_6F_5 rings are static in the limiting low-temperature spectrum, but exhibit a similar dependence upon temperature ($\Delta G^\ddagger_{253} = 47.1$ and 48.3 $\text{kJ}\cdot\text{mol}^{-1}$, respectively, for the *o*-F, see Experimental Section for details).

The structure proposed for these **15**–**17** binuclear complexes has been confirmed by X-ray crystallography, using a single crystal of **17**, obtained from slow diffusion of *n*-hexane into a solution of **17** in CHCl_3 at room temperature (see Figure 6). Relevant distances and angles are shown in Table 2. Complex **17** crystallizes in the centrosymmetric group $P\bar{1}$, with both enantiomeric cations at the Ru center, *S* and *R*, present in the unit cell, showing the expected piano-stool type geometry at the ruthenium center and square-planar at the platinum atom. The chelate bite angle $\text{Cl}(1)\text{-Ru}(1)\text{-P}(1)$ ($87.48(4)^\circ$) and the angles $\text{P}(1)\text{-Ru}(1)\text{-P}(2)$ ($94.01(4)^\circ$) and $\text{P}(2)\text{-Ru}(1)\text{-Cl}(1)$ ($89.03(4)^\circ$) are similar to those found in $[(\text{PPh}_2\text{C}\equiv\text{CPh})\text{Cp}^*\text{Ru}(\mu\text{-Cl})(\mu\text{-PPh}_2\text{C}\equiv\text{CPh})\text{Pt}(\text{C}_6\text{F}_5)_2]$, **A**. The $\text{Ru}\text{-P}(1)$ bridging length is identical within the experimental error ($2.3390(10)$ \AA) to the terminal $\text{Ru}\text{-P}(2)$ distance ($2.3346(11)$ \AA) and comparable to those found in cation **7**⁺ ($2.3278(12)$, $2.3451(11)$ \AA). The $\text{Pt}\text{-C}(\text{alkyne})$ bond distances ($2.188(4)$ and $2.229(4)$ \AA), the angle at the bridging chlorine atom ($\text{Ru}(1)\text{-Cl}(1)\text{-Pt}(1)$ $116.22(4)^\circ$), and the $\text{Ru}\text{-Pt}$ separation (4.094 \AA) are similar to those found in the

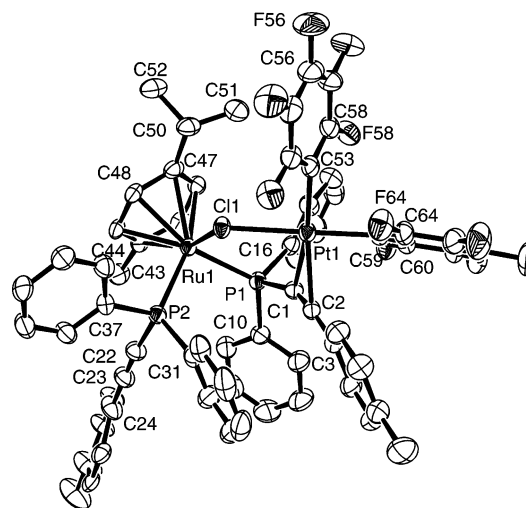


Figure 6. Molecular structure of the cation $[(\eta^6\text{-}p\text{-cymene})\{\text{PPh}_2\text{C}\equiv\text{C}(4\text{-CH}_3)\text{C}_6\text{H}_4\}\text{Ru}(\mu\text{-Cl})\mu\text{-}1\kappa\text{P}:\eta^2\text{-PPh}_2\text{C}\equiv\text{C}(4\text{-CH}_3)\text{C}_6\text{H}_4\}\text{Pt}(\text{C}_6\text{F}_5)_2](\text{OTf})$ in **17**. Ellipsoids are drawn at the 50% probability level. Hydrogen atoms have been omitted for clarity.

neutral bimetallic complex **12a**. Finally, coordination of the acetylenic fragment $\text{C}(1)\text{-C}(2)$ to Pt has a perceptible effect on both the bond length ($1.241(6)$ \AA in $\text{C}(1)\equiv\text{C}(2)$ vs $1.191(6)$ \AA in $\text{C}(22)\equiv\text{C}(23)$) and the linearity of the acetylenic group. Angles at $\text{C}(1)$ and $\text{C}(2)$ have values of $159.4(4)^\circ$ and $166.0(4)^\circ$, respectively, compared with $175.0(4)^\circ$ (angle at $\text{C}(22)$) and $179.0(5)^\circ$ (angle at $\text{C}(23)$) on the uncoordinated acetylenic fragment. For complex **16** no electrochemical response was observed from -1.8 to $+1.8$ V. By contrast, the binuclear compounds **15** and **17**, as observed for their cationic **6** and **8** precursors, again do not give electrochemical response in CH_2Cl_2 from 0 to 1.8 V. However, they show a quasi reversible reduction wave at -0.95 V for complex **15**, and at -1.016 V for complex **17**, and in the corresponding reverse scan one irreversible small anodic peak (-0.445 V **15**, -0.502 V **17**). Both the cathodic and the small anodic peak are notably more positive ($\Delta(\text{mV})$ 640 V (c), 577 V (a) **15**; 650 V (c), 542 V (a) **17**) compared to those observed in the precursors.

Conclusions

In conclusion, we report the synthesis and properties of some potentially useful neutral $[(\eta^6\text{-}p\text{-cymene})\text{RuCl}_2\text{-}$

(PPh₂C≡CR) (1–5) and cationic [(η⁶-*p*-cymene)RuCl(PPh₂C≡CR)₂]X (6–10) ruthenium complexes, bearing one or two diphenylphosphinoacetylene ligands, and investigate their reactivity toward the solvent species [*cis*-Pt(C₆F₅)₂(thf)₂]. ¹³C{¹H} NMR studies on the mononuclear complexes (1–10) suggest that the alkyne polarization on the PPh₂C≡CR ligand upon P-coordination is perceptibly higher in the cationic (6–10) complexes than in the neutral derivatives (1–5) and, in the latter, clearly enhanced with respect to those of free PPh₂C≡CR ligands. This spectroscopic behavior is entirely similar to that seen with the isoelectronic “M-(η⁵-C₅Me₅)” (M = Rh, Ir(III)) moieties and the PPh₂C≡CPh ligand, but contrasts with the fact that complexation of two PPh₂C≡CPh to the neutral “Ru(η⁵-C₅Me₅)Cl” fragment has been observed to have no effect on the alkyne polarization. We have shown that the neutral complexes react with [*cis*-Pt(C₆F₅)₂(thf)₂] to yield heterobimetallic compounds (11a–14a), stabilized in the solid state by a (μ-Cl)(μ-PPh₂C≡CR) bridging system, as has been confirmed by X-ray crystallography on complex 12a. In solution, these neutral bimetallic Ru(II)-Pt(II) complexes exist as a mixture of isomers (μ-Cl)(μ-PPh₂C≡CR) 11a–14a/(μ-Cl)₂ 11b–14b, which interconvert slower than the NMR time scale. It has been observed that the heteromixed bridged isomers type a are more favorable in chloroform than in acetone, but are disfavored at higher temperatures. The existence of only one isomer (a) in the solid state with the “(η⁶-arene)RuCl₂” fragment contrasts with the presence of both isomers (a + b, 1:1) previously observed with the isoelectronic “Ir(η⁵-C₅Me₅)Cl₂” unit or the doubly chloride-bridged isomer (b) seen with the “Rh(η⁵-C₅Me₅)Cl₂” moiety. Chiral cationic bimetallic d⁶-d⁸ complexes [(η⁶-*p*-cymene)(PPh₂C≡CR)Ru(μ-Cl)(μ-1κ^P:η²-PPh₂C≡CR)Pt(C₆F₅)₂](OTf) (15–17) have also been prepared starting from the cationic mononuclear complexes 6–8 and the synthon “*cis*-Pt(C₆F₅)₂”. In contrast to related chiral neutral isomers 11a–14a, the heterobridged system, in these cationic 15–17 compounds, was found to be stable in solution, making both halves of the *p*-cymene ligand nonequivalent. Finally, as is often found in other fluoroaryl complexes of Pt, the rotation of the C₆F₅ groups around the Pt–C₆F₅ bond is clearly hindered in the limiting low-temperature ¹⁹F spectra of all bimetallic 11–17 complexes. Furthermore, the presence of different ligands *trans* to the C₆F₅ rings in isomers 11a–14a and complexes 15–17 usually induces different rotation energy barriers for the C₆F₅ groups.

Experimental Section

C, H, and N analyses, conductivities (acetone, ca. 5 × 10⁻⁴ mol·L⁻¹), and IR and NMR spectroscopies were performed as described elsewhere,⁴⁸ the temperature of the routine NMR being 293 K. Literature methods were employed to prepare [Ru(η⁶-*p*-cymene)Cl₂]₂⁵¹ and [Pt(C₆F₅)₂(thf)₂]⁶³ complexes and

(59) Forniés, J.; Gómez, J.; Lalinde, E.; Moreno, M. T. *Chem. Eur. J.* **2004**, *10*, 888.

(60) Berenguer, J. R.; Forniés, J.; Lalinde, E.; Martín, A.; Serrano, B. *J. Chem. Soc., Dalton Trans.* **2001**, 2926.

(61) Ara, I.; Berenguer, J. R.; Eguizabal, E.; Forniés, J.; Lalinde, E. *Organometallics* **2001**, *20*, 2686.

(62) Ara, I.; Berenguer, J. R.; Eguizabal, E.; Forniés, J.; Lalinde, E.; Martín, A. *Eur. J. Inorg. Chem.* **2001**, 1631.

(63) Usón, R.; Forniés, J.; Tomás, M.; Menjón, B. *Organometallics* **1985**, *4*, 1912.

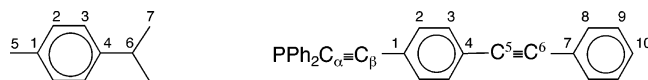


Figure 7. Labeling scheme for the carbon atoms in *p*-cymene and arylolethynylphosphine.

PPh₂C≡CR ligands (R = Ph,⁴⁹ ^tBu,⁴⁹ Tol⁵⁰). The novel alkynylphosphines PPh₂C≡CC₆H₄C≡CC₆H₅ and PPh₂C≡CC₆H₄CN used in this work have been prepared following the general procedure described by Carty et al.,⁴⁹ and their analytical and spectroscopic data are included in this work.

Cyclic voltammetric studies were performed using an EG&G model 283 potentiostat/galvanostat. The three-electrode system consists of a working platinum disk electrode, an auxiliary platinum wire electrode, and a saturated calomel reference (SCE). The measurements were carried out in anhydrous CH₂-Cl₂ solution under N₂ in the test compounds and 0.1 M in (NBu₄)[PF₆] as supporting electrolyte. The values are given versus FeCp₂^{+/}/FeCp₂ under the experimental conditions employed.

Figure 7 shows the labeling scheme for the carbon atoms in the *p*-cymene and in the arylolethynylphosphine.

Data for PPh₂C≡C(4-C≡CPh)C₆H₄. Yield: 72%. Anal. Calcd for C₂₈H₁₉P: C, 87.03; H, 4.96. Found: C, 86.90; H, 4.74. MS ES(+): *m/z* 389 [M + 3H]⁺ 16%; 387 [M + H]⁺ 4%; 285 [M - (C≡CPh)]⁺ 100%. IR (cm⁻¹): ν(C≡C) 2166 (m), 2152 (m). ¹H NMR (δ, CDCl₃): 7.66 (3H), 7.49 (8H), 7.34 (8H) (aromatic, C₆H₅ and C₆H₄). ¹³C{¹H} NMR (δ, CDCl₃): 136.2 (d, ¹J_{C-P} = 6.3, *i*-C, Ph); 132.7 (d, ²J_{C-P} = 21.0, *o*-C, Ph); 131.8 (d, ⁴J_{C-P} = 1.4, C₂, C₆H₄); 131.75 (C⁸, C₆H₅); 131.6 (d, ⁴J_{C-P} = 2.6, *p*-C, Ph); 129.2 (C³, C₆H₄); 128.8 (d, ³J_{C-P} = 7.7, *m*-C, Ph); 128.6 (C¹⁰, C₆H₅); 128.5 (C⁹, C₆H₅); 123.9 (C⁷, C₆H₅); 123.2 (d, ³J_{C-P} = 4.5, C¹, C₆H₄); 122.6 (C⁴, C₆H₄); 107.4 (d, ²J_{C-P} = 4.0, C_β); 91.8, 91.4 (C⁵=C⁶); 89.2 (d, ¹J_{C-P} = 11.1, C_ω). ³¹P{¹H} NMR (δ, CDCl₃): -33.27 (s).

Data for PPh₂C≡C(4-CN)C₆H₄. Yield: 26%. Anal. Calcd for C₂₁H₁₄NP: C, 81.02; H, 4.53; N, 4.50. Analyses of several samples always give lower values than expected: 76.23; 4.11; 3.58. MS ES(+): *m/z* 312 [M + H]⁺ 21%; 130 [M - Ph - C₆H₄-CN - 2H]⁺ 100%. IR (cm⁻¹): ν(CN) 2227 (s); ν(C≡C) 2172 (m). ¹H NMR (δ, CDCl₃): 7.62 (8H), 7.37 (6H) (CH, Ph). ¹³C{¹H} NMR (δ, CDCl₃): 135.3 (d, ¹J_{C-P} = 6.2, *i*-C, Ph); 132.7 (d, ²J_{C-P} = 21.1, *o*-C, Ph); 132.2 (d, ⁴J_{C-P} = 1.4, *p*-C, Ph); 132.1 (C², C₆H₄CN); 129.4 (C³, C₆H₄CN); 128.8 (d, ³J_{C-P} = 7.7, *m*-C, Ph); 127.5 (d, ³J_{C-P} = 1.1, C¹, C₆H₄CN); 118.4 (CN); 112.1 (C⁴, C₆H₄CN); 105.6 (d, ²J_{C-P} = 3.0, C_β); 91.7 (d, ¹J_{C-P} = 12.5, C_ω). ³¹P{¹H} NMR (δ, CDCl₃): -33.48 (s).

Synthesis of [(η⁶-*p*-cymene)RuCl₂(PPh₂C≡CR)] (R = Ph 1, ^tBu 2, Tol 3, C₆H₄C≡CC₆H₅ 4). **General Procedure. A solution of [(η⁶-*p*-cymene)RuCl₂]₂ (0.20 g, 0.33 mmol) in acetone (10 mL) was treated with two molar equivalents of the corresponding PPh₂C≡CR, and the mixture was stirred for ca. 45 min. The resulting orange solid was isolated by filtration, washed with diethyl ether (or ethanol in case of complex 4), and dried under vacuum.**

Data for 1. Yield: 84%. Anal. Calcd for C₃₀Cl₂H₂₉PRu: C, 60.81; H, 4.93. Found: C, 60.86; H, 4.85. MS ES(+): *m/z* 559 [M - Cl]⁺ 100%. IR (cm⁻¹): ν(C≡C) 2171 (s); ν(Ru-Cl) 295 (w), 283 (w). ¹H NMR (δ, CDCl₃): 8.04 (4H), 7.64 (2H), 7.5–7.36 (9H) (Ph); 5.33, 5.26 (AA'BB' system, J_{H-H} = 5.7, 4H, C₆H₄, *p*-cym); 2.94 (sept, J_{H-H} = 6.9, 1H, CH, ⁱPr); 1.98 (s, 3H, CH₃-C₆H₄); 1.17 (d, J_{H-H} = 6.9, 6H, CH₃, ⁱPr). ¹³C{¹H} NMR (δ, CDCl₃): 133.2 (d, ²J_{C-P} = 10.4, *o*-C, Ph); 132.12 (d, ¹J_{C-P} = 5.4, *i*-C, Ph); 132.1 (d, ⁴J_{C-P} = 1.5, *o*-C, C≡CPh); 130.4 (d, ⁴J_{C-P} = 2.7, *p*-C, Ph); 130.3 (p-C, C≡CPh); 128.7 (*m*-C, C≡CPh); 127.9 (d, ³J_{C-P} = 10.9, *m*-C, Ph); 120.9 (d, ³J_{C-P} = 3, *i*-C, C≡CPh); 109.4 (d, ²J_{C-P} = 1.3, C⁴, *p*-cym); 109.0 (d, ²J_{C-P} = 11.7, C_β); 96.1 (C¹, *p*-cym); 90.5 (d, ²J_{C-P} = 4.4, C³, *p*-cym); 86.7 (d, ²J_{C-P} = 6, C², *p*-cym); 83.6 (d, ¹J_{C-P} = 89.4, C_ω); 30.3 (C⁶, *p*-cym); 21.9 (C⁷, *p*-cym); 17.6 (C⁵, *p*-cym). ³¹P{¹H} NMR (δ, CDCl₃): -2.17 (s). E_p^a = 0.72 V (reversible).

131.03 (AXX', $^1J_{C-P} + ^3J_{C-P} = 56$, *i*-C, Ph); 130.5 (*p*-C, Ph); 129.6 (CH, Tol); 129.1 ("t", $^3J_{C-P} + ^5J_{C-P} = 11.6$, *m*-C, Ph); 128.2 ("t", $^3J_{C-P} + ^5J_{C-P} = 11.3$, *m*-C, Ph); 118.0 (C⁴, *p*-cym); 116.9 ("t", $^3J_{C-P} + ^5J_{C-P} = 2.8$, C¹, Tol); 113.9 (AXX', $^2J_{C-P} + ^4J_{C-P} = 14.3$, C_β); 101.4 (C¹, *p*-cym); 99.1 (t, $^2J_{C-P} = 4.4$, C³, *p*-cym); 92.19 ($^2J_{C-P} = 4.5$, C², *p*-cym); 78.4 (AXX', $^1J_{C-P} + ^3J_{C-P} = 106.5$, C_ω); 31.1 (C⁶, *p*-cym); 21.8, 21.5 (CH₃, Tol and C⁷, *p*-cym); 17.2 (C⁵, *p*-cym). ¹⁹F NMR (δ, CDCl₃): -78.27 (s, CF₃). ³¹P{¹H} NMR (δ, CDCl₃): 4.77 (s). $E_p^c = -1.666$ V (irreversible); $E_p^a = -1.044$ V (irreversible, small).

Data for 9. Yield: 60%. Anal. Calcd for C₆₇ClF₃H₅₂O₃P₂-RuS: C, 67.47; H, 4.39; S, 2.69. Found: C, 67.79; H, 4.73; S, 2.24. Λ_M : 134 Ω⁻¹·cm²·mol⁻¹. MS ES(+): *m/z* 1044 [M - OTf]⁺ 97%; 994 [M - OTf - Cl - CH₃]⁺ 100%; 909 [M - OTf - cym]⁺ 18%; 657 [M - OTf - PP₂C≡CC₆H₄C≡CC₆H₅]⁺ 86%. IR (cm⁻¹): ν(C≡C) 2171 (s); ν(OTf) 1264 (s), 1224 (s), 1154 (s), 1031 (s); ν(Ru-Cl) 254 (w). ¹H NMR (δ, CDCl₃): 8.1, 7.8, 7.49, 7.32, 7.11 (m, 38H, CH, Ph); 5.80 (d), 5.26 (d) ($J_{H-H} = 5.7$, 4H, C₆H₄, *p*-cym); 2.57 (sept, $J_{H-H} = 7.0$, 1H, CH, ⁱPr); 2.26 (s, 3H, CH₃-C₆H₄); 1.14 (d, $J_{H-H} = 7.0$, 6H, CH₃, ⁱPr). ¹³C{¹H} NMR (δ, CDCl₃): 134.6 (AXX', $^1J_{C-P} + ^3J_{C-P} = 58.6$, *i*-C, Ph); 132.5-128.3 (aromatics); 126.1, 122.6 (C⁴ and C⁷, phosphine); 119.4 (C¹, phosphine); 112.7 (AXX', $^2J_{C-P} + ^4J_{C-P} = 13.3$, C_β); 102.0 (C⁴, *p*-cym); 98.6 (C¹, *p*-cym); 93.2 (C³, *p*-cym); 92.8 (C⁵≡C⁶); 88.6 (C⁵≡C⁶); 88.5 (C², *p*-cym); 80.5 (AXX', $^1J_{C-P} + ^3J_{C-P} = 104$, C_ω); 31.1 (C⁶, *p*-cym); 21.6 (C⁷, *p*-cym); 17.5 (C⁵, *p*-cym). ¹⁹F NMR (δ, CDCl₃): -78.27 (s, CF₃). ³¹P{¹H} NMR (δ, CDCl₃): 6.95 (s). Electrode potential: no response was observed from -1.8 to 1.8 V.

Synthesis of [RuCl(η⁶-*p*-cymene)(PPh₂C≡CC₆H₄CN)₂]-PF₆ (10). A 0.10 g sample of [(*p*-cymene)RuCl₂(PPh₂C≡CC₆H₄CN)] (0.16 mmol) was stirred with 0.06 g (0.16 mmol) of TlPF₆ and 0.05 g of PPh₂C≡CC₆H₄CN (0.16 mmol) in acetone. After 90 min the mixture was evaporated to dryness, treated with CH₂Cl₂, and filtered through Celite. The resulting red solution was evaporated to dryness and treated with diethyl ether, affording **10** as an orange solid. Yield: 96.7%. Anal. Calcd for C₅₂ClF₆H₄₂N₂P₃Ru·CH₂Cl₂: C, 56.67; H, 3.95; N, 2.49. Found: C, 56.23; H, 3.91; N, 2.14. (The presence of CH₂Cl₂ has been observed by ¹H NMR spectroscopy.) Λ_M : 133 Ω⁻¹·cm²·mol⁻¹. MS ES(+): *m/z* 893 [M - PF₆]⁺ 16%; 682 [Ru(cym)₂(PPh₂C≡CC₆H₄CN)]⁺ 100%. IR (cm⁻¹): ν(C≡N) 2228 (m); ν(C≡C) 2176 (s); ν(PF₆) 839 (vs); ν(Ru-Cl) 288 (w). ¹H NMR (δ, CDCl₃): 7.85-7.06 (m, 28H, CH, Ph); 5.59, 5.46 (AA'BB' system, $J_{H-H} = 5.4$, 4H, C₆H₄, *p*-cym); 2.75 (sept, $J_{H-H} = 6.9$, 1H, CH, ⁱPr); 1.98 (s, 3H, CH₃-C₆H₄); 1.2 (d, $J_{H-H} = 6.9$, 6H, CH₃, ⁱPr). ¹⁹F NMR (δ, CDCl₃): -71.42 (d, $J_{P-F} = 714.7$, PF₆). ³¹P{¹H} NMR (δ, CDCl₃): -144.15 (sept, $J_{P-F} = 714.7$, PF₆). ³¹P{¹H} NMR (δ, CDCl₃): 3.31 (s). The ¹³C{¹H} NMR spectrum could not be obtained because it decomposes in solution. Electrode potential: no response was observed from -1.8 to 1.8 V.

Synthesis of [(η⁶-*p*-cymene)ClRu(μ-Cl)(μ-PPh₂C≡CR)-Pt(C₆F₅)₂] (Xa) (R = Ph, X = 11; R = ^tBu, X = 12; R = Tol, X = 13; R = C₆H₄C≡CC₆H₅, X = 14). General Procedure. Solutions of [(η⁶-*p*-cymene)RuCl₂(PPh₂C≡CR)] (R = Ph **1**, ^tBu **2**, Tol **3**, C₆H₄C≡CC₆H₅ **4**) in CH₂Cl₂ (10 mL) were treated with an equimolar amount of [*cis*-Pt(C₆F₅)₂(thf)₂]. In each case, the resulting solution was stirred for 10 min and evaporated to dryness. Addition of diethyl ether yielded complexes **11a**-**14a** as red (**11a**, **13a**), salmon pink (**12a**), and brown (**14a**) solids. Although in the solid state only complexes **Xa** (X = **11**-**14**) are present, in solution the NMR data indicate the presence of an equilibrium between the isomers **Xa** and [(η⁶-*p*-cymene)(PPh₂C≡CR)Ru(μ-Cl)₂Pt(C₆F₅)₂], **Xb** (X = **11**-**14**). The following amounts of precursors were employed. For **11**: 0.10 g (0.17 mmol) of **1** with 0.11 g of [*cis*-Pt(C₆F₅)₂(thf)₂]. For **12**: 0.15 g (0.26 mmol) of **2** with 0.18 g of [*cis*-Pt(C₆F₅)₂(thf)₂]. For **13**: 0.15 g (0.25 mmol) of **3** with 0.17 g of [*cis*-Pt(C₆F₅)₂(thf)₂]. For **14**: 0.10 g (0.15 mmol) of **4** with 0.11 g of [*cis*-Pt(C₆F₅)₂(thf)₂].

Data for 11a. Yield: 73%. Anal. Calcd for C₄₂Cl₂F₁₀H₂₉-PPtRu: C, 44.97; H, 2.61. Found: C, 44.74; H, 2.33. MS ES- (+): *m/z* 1149 [M + Na + 4H]⁺ 2%; 863 [M + Na - PPh₂C≡CPh+4H]⁺ 3%; 557 [M - Pt(C₆F₅)₂ - Cl]⁺ 100% (sample ionized with Na⁺). IR (cm⁻¹): ν(C≡C) 1989 (m); ν(C₆F₅)_X-sens 810 (m), 797 (m); ν(Ru-Cl) 305 (w), 258 (w). In solution, the observed ratio for the equilibrium **11a**/**11b** at room temperature is 55:45 in CDCl₃ and 25:75 in HDA. ¹H NMR (δ, CDCl₃): 8.18-7.11 (m, Ph, overlapped with those corresponding to phenyl protons of **11b**); 5.40 (s, C₆H₄, *p*-cym); 5.30 (s, vbr, C₆H₄, *p*-cym); 2.38 (sept, $J_{H-H} = 6.7$, CH, ⁱPr); 1.95 (s, CH₃-C₆H₄); 0.99 (d, $J_{H-H} = 6.7$, CH₃, ⁱPr). **11b**: 5.81, 5.76 (AA'BB' system, $J_{H-H} = 5.7$, C₆H₄, *p*-cym); 2.65 (sept, $J_{H-H} = 6.8$, CH, ⁱPr); 1.93 (s, CH₃-C₆H₄); 1.13 (d, $J_{H-H} = 6.8$, CH₃, ⁱPr). The two aromatic (CH, C₆H₄), and methyl (d, CH(CH₃)₂) resonances of *p*-cymene in **11a** broaden as the temperature is lowered, coalesce, and finally split: 5.73, 5.67, 5.27, 4.76 (CH); 0.97 (d, $J_{H-H} = 5.0$); 0.84 (d, $J_{H-H} = 4.9$). The ratio **11a**:**11b** observed at 223 K is 77:23. The T_c for the methyl groups is ca. 263 K ($\Delta G_{263}^\ddagger \approx 54.2$ kJ·mol⁻¹) and for the CH signals at 5.73 and 4.76 ppm ca. 283 K ($\Delta G_{283}^\ddagger \approx 53.8$ kJ·mol⁻¹). ¹⁹F NMR (δ, CDCl₃, 282.5 MHz): at 238 K, the ratio **11a**:**11b** is 75:25; -116.43 (d, $^3J_{Pt-O-F} \approx 345$), -117.18 (d, $^3J_{Pt-O-F} \approx 415$), -120.63 (d, $^3J_{Pt-O-F} \approx 400$), -123.00 (d, $^3J_{Pt-O-F} \approx 330$) (*o*-F); -160.13 (t, *p*-F); -161.30 (t, *p*-F); -162.92 (m), -164.22 (m) (1:3 *m*-F). **11b**: -119.28 (d, $^3J_{Pt-O-F} \approx 500$), -120.30 (d, $^3J_{Pt-O-F}$ cannot be determined) (*o*-F); -163.18 (t, *p*-F); -165.02 (m), -165.45 (m) (*m*-F). Upon heating, the *ortho* and *meta* signals of both complexes broaden and the relative concentration of **11b** increases. For **11a**, the signals at -117.18 and -120.63, corresponding to one C₆F₅ ring, coalesce at ca. 288 K ($\Delta G_{288}^\ddagger = 51.95$ kJ·mol⁻¹), while the signals at -116.43 and -123.00 coalesce at 298 K ($\Delta G_{298}^\ddagger = 52.2$ kJ·mol⁻¹). At the highest temperature recorded (308 K), no signals due to *o*-F have risen above the baseline. For **11b**, the two signals due to the *o*-F (as well as both of the signals due to *m*-F) broaden and coalesce at ca. 268 K (258 K for *m*-F; $\Delta G_{268}^\ddagger = 50.8$ kJ·mol⁻¹ for *o*-F, $\Delta G_{258}^\ddagger = 50.7$ kJ·mol⁻¹ for *m*-F). At 293 K: **11a**: the signals due to *o*-F are embedded in the baseline; -160.78 (t, *p*-F); -161.95 (t, *p*-F); -164.4 (s br, *m*-F); -164.79 (m, *m*-F). **11b**: -119.76 (s br, $^3J_{Pt-O-F} \approx 520$, *o*-F); -163.82 (t, *p*-F); -165.88 (m, *m*-F). ³¹P{¹H} NMR (δ, CDCl₃): 46.32 (s). **11b**: 8.03 (s). $E_p^a = 1.203$ V (irreversible).

Data for 12a. Yield: 76%. Anal. Calcd for C₄₀Cl₂F₁₀H₃₃-PPtRu: C, 43.61; H, 3.02. Found: C, 43.26; H, 3.08. MS ES- (+): *m/z* 1151 [M + 2Na + 3H]⁺ 35% (sample ionized with Na⁺). IR (cm⁻¹): ν(C≡C) 1990 (m); ν(C₆F₅)_X-sens 806 (m), 798 (m); ν(Ru-Cl) 308 (w), 229 (w). Complex **12a** is not very soluble in CDCl₃, although soluble enough to record the ¹H NMR spectrum. The observed ratio for the equilibrium **12a**/**12b** at room temperature is 60:40 in CDCl₃ and 30:70 in HDA. ¹H NMR (δ, CDCl₃): 8.41, 7.96, 7.82, 7.51 (m, Ph; overlapped with those corresponding to phenyl protons of **12b**); ~5.7 (br, C₆H₄, *p*-cym). This signal is obscured by the corresponding signals of **12b**); 5.46 (br), 5.21 (br), 4.60 (br) (C₆H₄, *p*-cym); 2.30 (sept, $J_{H-H} = 6.9$, CH, ⁱPr); 2.00 (s, CH₃-C₆H₄); 1.18 (d, $J_{H-H} = 6.9$), 1.16 (d, $J_{H-H} = 9.0$) (2 CH₃, ⁱPr); 0.82 (s, ^tBu). **12b**: 5.73 (AA'BB' system, $J_{H-H} \approx 5$, C₆H₄, *p*-cym); overlaps with the signal corresponding to one C₆H₄ proton of **12a**); 2.65 (sept, $J_{H-H} = 6.7$, CH, ⁱPr); 1.87 (s, CH₃-C₆H₄); 1.45 (s, ^tBu); 1.18 (d, $J_{H-H} = 7.2$, CH₃, ⁱPr). ¹³C{¹H} NMR (δ, HDA): only signals due to **12b** can be assigned unequivocally; 133.5 (d, $^2J_{C-P} = 11.17$, *o*-C, Ph); 132.2 (d, $^4J_{C-P} = 2.9$, *p*-C, Ph); 131.8 (d, $^1J_{C-P} = 56$, *i*-C, Ph); 129.6 (d, $^3J_{C-P} = 11.3$, *m*-C, Ph); 124.3 (d, $^2J_{C-P} = 12.2$, C_β); 110.1 (d, $^2J_{C-P} = 1.5$, C⁴, *p*-cym); 100.4 (C¹, *p*-cym); 91.4 (d, $^2J_{C-P} = 4.1$); 90.3 (d, $^2J_{C-P} = 4.8$) (C² and C³, *p*-cym); 71.2 ($J_{C-P} = 103$, tentatively assigned to C_ω); 31.5 (C⁶, *p*-cym); 30.5 (d, $^4J_{C-P} = 1.4$, C(CH₃)₃); 22.1 (C⁷, *p*-cym); 18.2 (C⁵, *p*-cym). ¹⁹F NMR (δ, HDA, 376.47 MHz): at 200 K the ratio **12a**/**12b** is ~30:70; -116.87 (m), -117.54 (m), -121.19 (m), -122.28 (m) (1:1:1:1, *o*-F) (platinum satellites are observed

$\nu(\text{C}_6\text{F}_5)_x\text{-sens}$ 808 (s br); $\nu(\text{Ru}-\text{Cl})$ 260 (w). $^1\text{H NMR}$ (δ , CDCl_3): 7.99, 7.68, 7.47, 7.36, 7.25, 7.18 (m, 20H, Ph); 5.91 (s br), 5.68 (d, $J_{\text{H-H}} = 5.7$), 5.29 (s br), 5.0 (d, $J_{\text{H-H}} = 5.3$) (4H, C_6H_4 , *p*-cym); 2.08 (m, 1H, CH, ^iPr); 2.00 (s, 3H, $\text{CH}_3\text{-C}_6\text{H}_4$); 1.53 (s, 9H, ^tBu); 1.08 (d, $J_{\text{H-H}} = 6.7$, 3H, CH_3 , ^iPr); 0.98 (d, $J_{\text{H-H}} = 6.7$, 3H, CH_3 , ^iPr); 0.82 (s, 9H, ^tBu). $^{19}\text{F NMR}$ (δ , CDCl_3 , 223 K): -78.68 (s, 3F, OTf); -115.11 (br, 1 *o*-F); -116.59 (br, 1 *o*-F); -121.60 (br, 1 *o*-F); -122.46 (br, 1 *o*-F) ($^3J_{\text{Pt-o-F}}$ cannot be assigned); -157.84 (br, 1 *p*-F); -159.03 (br, 1 *p*-F); -162.04 (br, 1 *m*-F); -162.72 (br, 3 *m*-F). Upon heating, the signals at -115.11 and -116.59, as well as the signals at -121.60 and -122.46, broaden and coalesce at ca. 253 K ($\Delta G_{253}^\ddagger = 47.1$ and 48.3 $\text{kJ}\cdot\text{mol}^{-1}$, respectively). At 293 K: -78.41 (s, 3F, OTf); -117.88 (d, $^3J_{\text{Pt-o-F}} \approx 350$, 2 *o*-F); -120.84 (d, $^3J_{\text{Pt-o-F}} \approx 390$, 2 *o*-F); -158.55 (t, 1 *p*-F); -159.64 (t, 1 *p*-F); -163.22 (m, 4 *m*-F). $^{31}\text{P}\{^1\text{H}\}$ NMR (δ , CDCl_3): 36.51 (d, $\mu\text{-P}$); 0.72 (d) ($^2J_{\text{P-P}} = 51.3$). Electrode potential: no response was observed from -1.8 to 1.8 V.

Data for 17. Yield: 71%. Anal. Calcd for $\text{C}_{65}\text{ClF}_{13}\text{H}_{48}\text{O}_3\text{P}_2\text{-PtRuS}$: C, 50.38; H, 3.12; S, 2.07. Found: C, 49.98; H, 2.76; S, 1.93. Λ_{M} : 121 $\Omega^{-1}\cdot\text{cm}^2\cdot\text{mol}^{-1}$. MS ES(+): m/z 1401 [$\text{M} - \text{OTf}]^+ 100\%$. IR (cm^{-1}): $\nu(\text{C}\equiv\text{C})$ 2170 (m); $\nu(\mu\text{-C}\equiv\text{C})$ 1972 (m); $\nu(\text{C}_6\text{F}_5)_x\text{-sens}$ 815 (m), 807 (m); $\nu(\text{Ru}-\text{Cl})$ 270 (w). $^1\text{H NMR}$ (δ , CDCl_3) 8.29, 7.91, 7.57, 7.40, 7.27, 6.97, 6.82, 6.63 (m, 28H, aromatics, Ph and Tol); 5.88 (s br, 1H), 5.75 (m, 2H), 4.83 (d, $J_{\text{H-H}} = 5.3$, 1H) (C_6H_4 , *p*-cym); 2.45 (s, 3H, CH_3 , Tol); 2.40 (m, 1H, CH, ^iPr); 2.26 (s, 3H, $\text{CH}_3\text{-C}_6\text{H}_4$), 2.24 (s, 3H, $\text{CH}_3\text{-C}_6\text{H}_4$) (Tol and *p*-cym); 1.10 (d, $J_{\text{H-H}} = 6.7$, 3H, CH_3 , ^iPr); 1.02 (d, $J_{\text{H-H}} = 6.6$, 3H, CH_3 , ^iPr). $^{19}\text{F NMR}$ (δ , CDCl_3 , 233 K): -78.65 (s, 3F, OTf); -115.52 (d, $^3J_{\text{Pt-o-F}} \approx 420$, 1 *o*-F); -117.35 (d, $^3J_{\text{Pt-o-F}} \approx 360$, 1 *o*-F); -120.64 (d, $^3J_{\text{Pt-o-F}} \approx 410$, 1 *o*-F); -123.35 (d, $^3J_{\text{Pt-o-F}} \approx 295$, 1 *o*-F); -158.25 (t, 1 *p*-F); -160.24 (t, 1 *p*-F); -162.23 (m, 1 *m*-F); -163.53 (m, 2 *m*-F); -163.97 (m, 1 *m*-F). Upon heating, the exterior *o*-F signals broaden and, finally, coalesce at 298 K ($\Delta G_{298}^\ddagger = 51.8$ $\text{kJ}\cdot\text{mol}^{-1}$). On the same line, two *m*-F signals located at -163.53 and -163.97 coalesce at ca. 263 K ($\Delta G_{263}^\ddagger \approx 51.7$ $\text{kJ}\cdot\text{mol}^{-1}$). At 293 K: -78.39 (s, 3F, OTf); -116.0 (v br, 1 *o*-F); -117.30 (d, $^3J_{\text{Pt-o-F}} \approx 365$, 1 *o*-F); -120.61 (d, $^3J_{\text{Pt-o-F}} \approx 405$, 1 *o*-F); -122.5 (v br, 1 *o*-F); -158.80 (t, 1 *p*-F); -160.92 (t, 1 *p*-F); -162.90 (m, 1 *m*-F); -163.91 (m, 1 *m*-F); -164.26 (m, 2 *m*-F). $^{31}\text{P}\{^1\text{H}\}$ NMR (δ , CDCl_3): 51.38 (d, $\mu\text{-P}$); 2.72 (d) ($^2J_{\text{P-P}} = 53.0$). $E_{\text{p}}^{\text{c}} = -1.016$ V (quasi reversible); $E_{\text{p}}^{\text{a}} = -0.502$ V (irreversible).

X-ray Crystallography. Table 1 reports details of the structural analyses for all complexes. Orange (**3**, **7**) or yellow (**17**) crystals were obtained by slow diffusion of *n*-hexane into a dichloromethane (**3**) or chloroform (**7**, **17**) solution of each compound at room temperature, while red crystals of **12a** were obtained, leaving an acetone solution of this complex to evaporate at room temperature. For complex **12a** one molecule of acetone and for complex **17** two molecules of CHCl_3 are found, respectively, in the asymmetric unit. X-ray intensity data were collected with a NONIUS kCCD area-detector diffractometer, using graphite-monochromated Mo $K\alpha$ radia-

tion. Images were processed using the DENZO and SCALEPACK suite of programs,⁶⁴ and the absorption correction was performed using SORTAV.⁶⁵ The structure of **12a**·(acetone) was solved by Patterson and Fourier methods using the DIRDIF92 program,⁶⁶ while the rest of the structures were solved by direct methods (**3**) or the Patterson method (**7**, **17**· 2CHCl_3) using the SHELXL-97 program.⁶⁷ The four structures were refined by full-matrix least squares on F^2 with SHELXL-97. All non-hydrogen atoms were assigned anisotropic displacement parameters, and all hydrogen atoms were constrained to idealized geometries fixing isotropic displacement parameters of 1.2 times the U_{iso} value of their attached carbon for the phenyl and methine hydrogens and 1.5 for the methyl groups. In the case of complex **17**, one phenyl group (C(24)–C(29)) presents a positional disorder, which could be refined over two positions with partial occupancy factors of 0.50. The absolute structure parameters for **7** and **12a**·(acetone) are -0.03(3) and 0.031(5), respectively. **12a**·(acetone), which crystallizes in the space group $P2_12_12_1$, shows the enantiomorphic *S* form in the crystallographic study presented in this paper (Figure 2). Nevertheless, one study carried out with another crystal chosen from the same crystalline sample has shown the enantiomer *R* for complex **12a**. The cation present in complex **17** also possesses a chiral center in the ruthenium atom, but in this case both enantiomers, *R* and *S*, are present in the unit cell (Figure 6 shows the enantiomer *R*). Finally, for complex **12a**, the low quality of the crystals does not allow the observation of reflections at high θ , and, also, two residual peaks (1.59 and 1.44 $\text{e}\cdot\text{\AA}^{-3}$) close to the Pt atom were observed, but with no chemical significance.

Acknowledgment. We wish to thank the Dirección General de Investigación, Spain, and the European Regional Development Fund (Projects BQU2002-03997-C02-01, 02, PGE-FEDER) and the Comunidad de La Rioja (APCI-2002/8) for financial support and grants to A.G. and M.B., respectively.

Supporting Information Available: Further details of the structure determinations of **3**, **7**, **12a**·(acetone), and **17**· 2CHCl_3 in CIF format. This material is available free of charge via the Internet at <http://pubs.acs.org>.

OM049676J

(64) Otwinowski, Z.; Minor, W. In *Methods in Enzymology*; Carter, C. V., Jr., Sweet, R. M., Eds.; Academic Press: New York, 1997; Vol. 276A, p 307.

(65) Blessing, R. H. *Acta Crystallogr.* **1995**, *A51*, 33.

(66) Beursken, P. T.; Beursken, G.; Bosman, W. P.; de Gelder, R.; Garcia-Granda, S.; Gould, R. O.; Smith, J. M. M.; Smykalla, C. *The DIRDIF92 program system*; Technical Report of the Crystallography Laboratory: University of Nijmegen: The Netherlands, 1992.

(67) Sheldrick, G. M. *SHELX-97, a program for the refinement of crystal structures*; University of Göttingen: Germany, 1997.